

Understanding the dynamics of biological and neural oscillator networks through mean-field reductions: a review

Christian Bick^{1,4}, Marc Goodfellow^{2,3,5}, Carlo R. Laing⁶, Erik Andreas Martens^{7,8}

1 Centre for Systems, Dynamics, and Control, University of Exeter, Exeter, United Kingdom

2 Department of Mathematics, College of Engineering, Mathematics, and Physical Sciences, University of Exeter, Exeter, United Kingdom

3 EPSRC Centre for Predictive Modelling in Healthcare, University of Exeter, Exeter, United Kingdom

4 Mathematical Institute, University of Oxford, Oxford, United Kingdom

5 Living Systems Institute, University of Exeter, Exeter, United Kingdom

6 School of Natural and Computational Sciences, Massey University, Auckland, New Zealand

7 Department of Applied Mathematics and Computer Science, Technical University of Denmark, 2800 Kgs. Lyngby, Denmark

8 Department of Biomedical Science, University of Copenhagen, 2200 Copenhagen N, Denmark

Abstract

Many biological and neural system can be seen as networks of interacting periodic processes. Importantly, the function of these networks depends on the collective dynamics: Synchrony of oscillations is probably amongst the most prominent examples of collective behavior and has been associated both with function and dysfunction. Understanding how network structure and interactions, as well as the microscopic properties of individual units, shape the emergent collective dynamics is critical to find factors that lead to malfunction. However, many biological systems such as the brain consist of a large number of dynamical units. Hence, their analysis has either primarily relied on simplified heuristic models on a coarse scale, or the analysis comes at a huge computational cost. Here we review recently introduced approaches—commonly known as the Ott–Antonsen and Watanabe–Strogatz reductions—that allow to simplify the analysis by bridging small and large scales: To obtain reduced model equations, a subpopulation in an oscillator network is replaced by a single variable that describes its collective state exactly. The resulting equations are next-generation models: Rather than being heuristic, they capture microscopic properties of the underlying system. At the same time, they are sufficiently simple to analyze without great computational effort. In the last decade, these reduction methods have become instrumental to understand how network structure and interaction shapes the collective dynamics and the emergence of synchrony. We review this progress based on concrete examples and outline possible limitations. Finally, we discuss how linking the reduced models with experimental data can guide the way towards the development of new treatment approaches, for example, for neural disease.

Author summary

The function or dysfunction of many biological systems, including the brain, depends on the collective dynamics of many oscillatory processes. But how is it possible to understand how the interaction gives rise to collective dynamics such as synchrony if there are millions of oscillators?

Here we review recent approaches that allow to replace a large number of individual oscillators by just a few collective variables, thereby simplifying the analysis tremendously. Importantly, these reductions describe the system dynamics exactly (rather than being heuristic or approximate), they capture microscopic properties of the individual oscillators, but are—due to their reduced nature—sufficiently simple to analyze. On the one hand, we give mathematical detail for the readers who are interested in understanding how the reduced equations are derived. On the other hand, we discuss concrete examples of how these tools have been used to simplify and solve long-standing problems in the dynamics of oscillator networks. A future challenge is to connect the mean-field reductions reviewed here with experimental data; solving this challenge will provide tools for developing new approaches to treat, for example, neural disease.

Introduction

Many systems in neuroscience and biology are governed on different levels by interacting periodic processes [1]. Networks of coupled oscillators provide models for such systems. Each node in the network is an oscillator (a dynamical process) and the network structure encodes which oscillators interact with each other [2]. In neuroscience, individual oscillators could be single neurons in microcircuits or neural masses on a more macroscopic level [3]. Other prominent examples in biology include cells in heart tissue [4], flashing fireflies [5], gait patterns of animals [6] or humans [7], cells in the suprachiasmatic nucleus in the brain generating the master clock for the circadian rhythm [8–10], suspensions of yeast cells undergoing metabolic oscillations [11, 12], and life cycles of phytoplankton in chemostats [13].

The function—or dysfunction—of these networks depends on the *collective dynamics* of the interacting oscillatory nodes. Hence, one major challenge is to understand how the underlying network shapes these collective dynamics. In particular, one would like to understand how the interplay of network properties (for example, connectivity and strength of interactions) and properties of the individual nodes shape the emergent dynamics. The question of relating network structure and dynamics is particularly pertinent in the study of large-scale brain dynamics, for example one can investigate how emergent functional connectivity (a dynamical property) arises from specific structural connectomes [14, 15], and how each of these relates to cognition or disease. Progress in this direction not only aims to identify how healthy or pathological dynamics is linked to the network structure, but also to develop new treatment approaches [16–18].

One of the most prominent collective behaviors of an oscillator network occurs when nodes synchronize and oscillate in unison [19–21]; indeed, most of the examples given above display synchrony in some form which appears to be essential to the proper functioning of biological life processes. Here we think of synchrony in a general way: It can come in many varieties, including *phase synchrony* where the state of different oscillators align exactly, or *frequency synchrony* where the oscillators' frequencies coincide. Synchrony may be *global* across the entire network or *localized* in a particular part—the rest of the network being nonsynchronized—thus giving rise to *synchrony patterns*. How exactly the dynamics of synchrony patterns in an oscillator network relate to its functional properties is still not fully understood. In the brain, there are a wide range of rhythms but the presence of dominant rhythms in different frequency bands indicate that some level of synchrony is common at multiple scales [22, 23]. Indeed, synchrony has been associated with solving functional tasks including memory [24], computational functions [25], cognition [26], attention [27, 28], control of gait and motion [29], or breathing [30, 31]. At the same time, abnormal synchrony patterns are associated with malfunction in disorders such as epilepsy and Parkinson's disease [32–34].

Using a detailed model of each node and a large number of nodes in the network, relating net-

work structure and dynamics is a daunting task. Hence simplifying analytical reduction methods are needed that, rather than being purely computational, yield a mechanistic understanding of the inherent processes leading to a certain dynamic macroscopic behavior. If many biologically relevant state variables are considered in a microscopic model, each node is represented by a large dynamical system by itself. Hence, a common approach is to simplify the description of each oscillatory node to its simplest form, a *phase oscillator*; in the reduced system the state of each oscillator is given by a single periodic phase variable that captures the state of the periodic process. In this case, biologically relevant details are captured by the evolution of the phase variable and its interaction with the phases of the other nodes. There are two important ways to get to a phase description of an oscillator network, both of which are common tools used, for example, in computational neuroscience; see [35] for a recent review. First, under the assumption of weak coupling one can go through a process of phase reduction to obtain a phase description [36–41]. Second, one can—based on the biophysical properties of the system—impose a phase model such as the Kuramoto model [42] or a network of Theta neurons [43].

The main topic of this paper is a review of recent advances that allow a further reduction in the complexity of the problem: Under certain assumptions, it is possible to replace a large number of nodes by a *collective* or *mean-field variable*. We focus here on phase oscillator networks that are organized into distinct (sub)populations because of their practical importance¹. In the neuroscientific context, each subpopulation may represent different populations of neurons that may exhibit temporal patterns of synchronization or activity [14, 15, 46]. The mean-field reductions we present allow one to replace each subnetwork by a (low-dimensional) set of collective variables to obtain a set of dynamical equations for these variables. This set of mean-field equations describes the system exactly. For the classical Kuramoto model, which is widely used to understand synchronization phenomena, we will see below that the collective state is captured by a two-dimensional mean-field variable that encodes the synchrony of the population. Reducing to a set of mean-field equations provides a simplified—but often still sufficiently complex—description of the network dynamics that can be analyzed by using dynamical systems techniques [47]. Compared to heuristic macroscopic models, the reduced equations capture microscopic properties of individual oscillators; because of this property these reduced equations have been referred to as being *next-generation models* [48]. Moreover, we will outline in this review how these reduction techniques reviewed here have been instrumental in the last decade to illuminate how the network properties relate to the dynamics, including the emergence of synchrony patterns.

There are many important questions and aspects that we cannot touch upon in this review, and we refer to already existing reviews and literature instead. First, we only consider oscillator networks where each (microscopic) node has a first-order description by a single phase variable. We will not cover other microscopic models such as second-order phase oscillators or oscillators with a phase and amplitude² which can give rise to richer dynamics. Second, we do not comment on the validity of a phase reduction; for more information see for example [38, 41]. Third, synchrony patterns relate to “chimera states,” which have attracted a significant amount of attention. While we mention results relevant to our discussions, we refer to [49–51] for recent reviews on chimeras. Fourth, the results mentioned here relate to results from network science [52, 53]. In particular, properties of the graph underlying the dynamical network relate to synchronization dynamics [54–56]. Moreover, we also typically assume that the network structure is static and does not evolve over time. However, time-dependent network structures are clearly of interest—in particular in the context of plastic neural connectivity. An approach to these issues from the

¹Such networks may be thought of as “networks of networks” [44, 45].

²Note, however, that the mesoscopic description in terms of collective variables of each subnetwork can have a “phase” and “amplitude” such as the mean phase and the amount of synchrony.

perspective of network science are temporal networks [57] while asynchronous networks take a more dynamical point of view; see [58] and references therein. Fifth, we restrict ourselves to deterministic dynamics where noise is absent. From a mathematical point of view, noise can simplify the analysis and recent results show that similar reduction methods apply [59]. Finally, it is worth noting that other reduction approaches for oscillator networks have recently been explored [60–62].

This review is written with a diverse readership in mind, ranging from mathematicians to computational biologists who want to use the reduced equations for modelling. Hence, we now outline how to read this paper. The next section sets the stage (and should therefore be read by all readers) since we introduce the notion of a sinusoidally coupled network and summarize the main oscillator models we relate to throughout the paper; these include the Kuramoto model and networks of Theta neurons. In the third section, we give a general theory for the mean-field reductions and discuss their limitations: The methods include the Ott–Antonsen reduction for the continuum limit of nonidentical oscillators and the Watanabe–Strogatz reduction for finite or infinite networks of identical oscillators. The section includes some level of mathematical detail to understand the ideas behind the derivation of the reduced equations (mathematically dense sections are marked with the symbol “*”, so they may be omitted if required [63]). If you are mainly interested in applying the reduced equations, you may want to skip ahead to the sections [Ott–Antonsen equations for commonly used oscillator models](#) and [Watanabe–Strogatz equations for commonly used oscillator models](#), which summarize the reduced equations for the models we study throughout the paper. In the fourth section, we apply the reductions and emphasize how they are useful to understand how synchrony and synchrony patterns emerge in such oscillator networks. This includes a number of concrete examples. Since most of these considerations are theoretical and computational, we discuss how the mean-field reductions can be linked with experimental data in the last section. We conclude with some remarks and highlighting a number of open problems.

List of symbols

\mathbb{N}	The positive integers
\mathbb{T}	The circle of all phases $[0, 2\pi)$
\mathbb{C}	The complex numbers
i	Imaginary unit $\sqrt{-1}$
$\text{Re}(w), \text{Im}(w)$	Real and imaginary part of a complex number w
M	Number of oscillator populations in the network
σ, τ	Population indices in $\{1, \dots, M\}$
N	Number of oscillators in each population
k, j, l, \dots	Oscillator indices in $\{1, \dots, N\}$
$\theta_{\sigma,k}$	Phase of oscillator k in population σ
$\kappa, \kappa^{\text{GJ}}, \kappa^{\text{g}}$	Coupling strength between neural oscillators
Z_σ	Kuramoto order parameter of population σ
R_σ	The level of synchrony $ Z_\sigma $ of population σ
z_σ, Ψ_σ	Bunch variables of population σ
\dot{x}	The time derivative $\frac{dx}{dt}$ of the quantity x

Sinusoidally coupled phase oscillator networks

We consider phase oscillator networks where the state of each node is given by a single phase variable. These networks may be obtained through a phase reduction or may be abstract mod-

els in their own right as in the case of the Theta neuron below. More specifically, consider a population σ of N oscillators where the state of oscillator k is given by a phase $\theta_{\sigma,k} \in \mathbb{T}$; if there is only a single population, we drop the index σ . Without input, the phase of each oscillator (σ, k) advances at its *intrinsic frequency* $\omega_{\sigma,k} \in \mathbb{R}$. Input to oscillator (σ, k) is determined by a field $H_{\sigma,k}(t) \in \mathbb{C}$ which is modulated by a sinusoidal function; this field could be external driving or network interactions between oscillators both within population σ or other populations τ . In other words, we consider oscillator networks whose phases evolve according to

$$\dot{\theta}_{\sigma,k} = \omega_{\sigma,k} + \text{Im}(H_{\sigma,k} e^{-i\theta_{\sigma,k}}). \quad (1)$$

Since the effect of the field is mediated by a function with exactly one harmonic, we call the oscillator populations *sinusoidally coupled*.

While we allow the intrinsic frequency and the driving field to depend on the oscillator to a certain extent (i.e., they are nonidentical), we will henceforth also assume that all oscillators within any given population σ otherwise are *indistinguishable*: This means that the properties of each oscillator in a given population are determined by the same distribution. Specifically, suppose that the properties of each oscillator are determined by a parameter $\eta_{\sigma,k}$ —for example, the excitability in the case of a Theta neuron we describe below. Now let both the intrinsic frequencies and the field be functions of this parameter, that is, $\omega_{\sigma,k} = \omega_{\sigma}(\eta_k)$, $H_{\sigma,k}(t) = H_{\sigma}(t; \eta_k)$. The oscillators of a given population are indistinguishable if, for a given population σ , all η_k are random variables sampled from a single probability distribution with density $h_{\sigma}(\eta)$. In the special case that all η_k are equal (in this case h_{σ} is a delta-distribution) the oscillators are *identical*.

Phase oscillator networks of the form (1) include a range of well-known (and well-studied) models. In the following we discuss some important examples that we will come back to throughout this paper.

The Kuramoto model

Kuramoto originally studied synchronization in a network of N globally coupled nonidentical units [64]; see [65] for an excellent survey of the problem and its historical background. Thus, there is only a single population of oscillators with phases θ_k , $k = 1, \dots, N$, and we drop the population parameter σ . The macroscopic or average dynamic behavior of the population is characterized by Kuramoto’s (complex-valued) order parameter

$$Z = R e^{i\phi} = \frac{1}{N} \sum_{j=1}^N e^{i\theta_j}. \quad (2)$$

The level of synchronization of the oscillator population is described by the magnitude R of the order parameter, see Fig. 1: On the one hand, $R = 1$ if and only if all oscillators are *phase synchronized*, that is, $\theta_k = \theta_j$ for all k and j ; on the other hand, we have $R = 0$ for example if the oscillators are evenly distributed around the circle. The argument ϕ of the Kuramoto order parameter Z describes the “average phase” of all oscillators, that is, it describes the average position of the oscillator crowd on the circle of phases.

Kuramoto originally investigated the *onset of synchronization* in a network of oscillators whose phases evolve according to

$$\dot{\theta}_k = \omega_k + \frac{K}{N} \sum_{j=1}^N \sin(\theta_j - \theta_k) \quad (3)$$

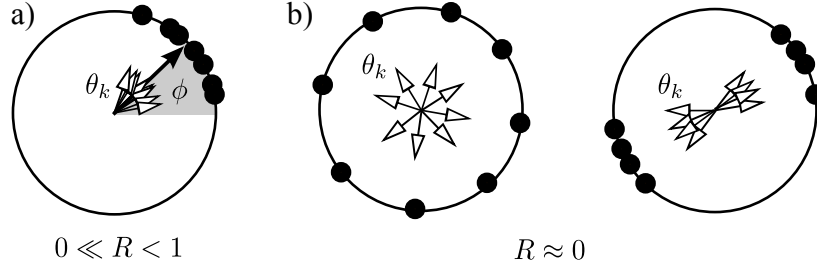


Fig 1. The Kuramoto order parameter (2) encodes the level of synchrony of a phase oscillator population. The state of each oscillator is given by a phase θ_k (black dot, empty arrow) on the circle \mathbb{T} . Panel (a) shows a configuration with high synchrony where $R = |Z| \approx 1$. Panel (b) shows two configurations with $R = |Z| \approx 0$: one where the oscillators are approximately uniformly distributed on the circle, the other one where they are organized into two clusters.

with distinct intrinsic frequencies ω_k following some frequency distribution. Here K is the coupling strength between oscillators and the coupling is mediated by the sine of the phase difference between oscillators. Thus, in the case of no coupling ($K = 0$) each oscillator advances with its intrinsic frequency ω_k . Kuramoto observed the following macroscopic behavior: For K small, the system converges to an incoherent stationary state with $R \approx 0$. As K is increased past a critical coupling strength K_c , the system settles down to a state with partial synchrony, $R > 0$. As the coupling strength is further increased, $K \rightarrow \infty$, oscillators become more and more synchronized, $R \rightarrow 1$.

The Kuramoto model (3) is an example of a sinusoidally coupled phase oscillator network. Using Euler's identity $e^{i\phi} = \cos(\phi) + i \sin(\phi)$, we have

$$\dot{\theta}_k = \omega_k + \text{Im} \left(\frac{K}{N} \sum_{j=1}^N e^{i(\theta_j - \theta_k)} \right) = \omega_k + \text{Im}(KZ e^{-i\theta_k})$$

with the Kuramoto order parameter Z as in (2). Hence, the Kuramoto model (3) is equivalent to (1) with $H = KZ$ and the interactions between oscillators are solely determined by the value of the Kuramoto order parameter Z . Such a form of network interaction is also called *mean-field coupling* since the drive H to a single oscillator is proportional to a mean formed from the states of all oscillators in the network.

Populations of Kuramoto–Sakaguchi oscillators

Sakaguchi generalized Kuramoto's model by introducing an additional phase-lag (or phase-frustration) parameter which approximates a time delay in the interactions between oscillators [49, 66]. While Sakaguchi originally considered a single population of oscillators, we here generalize to multiple interacting populations. Specifically, we consider the dynamics of M populations of N Kuramoto–Sakaguchi oscillators and the phase of oscillator k in population σ evolves according to

$$\dot{\theta}_{\sigma,k} = \omega_{\sigma,k} + \sum_{\tau=1}^M \frac{K_{\sigma\tau}}{N} \sum_{j=1}^N \sin(\theta_{\tau,j} - \theta_{\sigma,k} - \alpha_{\sigma\tau}) \quad (4)$$

where $K_{\sigma\tau} \geq 0$ is the *coupling strength* and $\alpha_{\sigma\tau}$ is the *phase lag* between populations σ and τ ³. The function $g_{\sigma\tau}(\phi) = K_{\sigma\tau} \sin(\phi - \alpha_{\sigma\tau})$ mediates the interactions between oscillators, and we refer to it as the *coupling function*; later on we will also briefly touch upon what happens if sine is replaced by a *general* periodic coupling function. As in the Kuramoto model, an important point is that the influence between oscillators (τ, j) and (σ, k) depends only on their phase *difference* (rather than explicitly on their phases)⁴. Thus, this form of interaction only depends on the relative phase between oscillator pairs rather than the absolute phases. An important consequence is that the dynamics of equations (4) do not change if we consider all phases in a different reference frame: For example, a reference frame rotating at (constant)⁵ frequency $\omega_f \in \mathbb{R}$ —corresponding to the transformation $\theta_{\sigma,k} \mapsto \theta_{\sigma,k} - \omega_f t$ —does not change the dynamics but shifts all intrinsic frequencies by ω_f .

The network (4) of M interacting populations of Kuramoto–Sakaguchi oscillators is a sinusoidally coupled oscillator network. The amount of synchrony in population σ is then determined by the Kuramoto order parameter (2) for population σ ,

$$Z_\sigma = \frac{1}{N} \sum_{j=1}^N e^{i\theta_{\sigma,j}}. \quad (5)$$

Combining coupling strength and phase lag, we define the complex interaction parameter $c_{\sigma\tau} := K_{\sigma\tau} e^{-i\alpha_{\sigma\tau}}$ between populations σ and τ . By the same calculation as above, the network (4) is equivalent to (1) with constant intrinsic frequencies $\omega_{\sigma,k}$ and drive

$$H_\sigma = \sum_{\tau=1}^M c_{\sigma\tau} Z_\tau \quad (6)$$

being a linear combination of the mean fields of the other populations.

Networks of Kuramoto–Sakaguchi oscillators have been used as models for synchronization phenomena. In neuroscience, individual oscillators can represent neurons [68] or large numbers of neurons in neural-masses [42, 69, 70]. In the framework of the model (4), the populations can be thought of as M neural masses. In contrast to models where neural masses only have a phase, here the macroscopic state of each population (neural mass) is determined by an amplitude (the level of synchrony $R_\sigma = |Z_\sigma|$) and a phase (the average phase $\phi_\sigma = \arg Z_\sigma$).

Theta and quadratic integrate and fire neurons

Theta neurons. The Theta neuron is the normal form of the saddle-node-on-invariant-circle (SNIC) or saddle-node-infinite-period (SNIPER) bifurcation [71], see Fig. 2: At the excitation threshold $I = 0$, a saddle and a node coalesce on an invariant circle (i.e., limit cycle of the neuron). It is a valid description of the dynamics of any neuron model undergoing this bifurcation, in some parameter neighborhood of the bifurcation. The Theta neuron is also a canonical Type 1 neuron [72].

Consider a single population of Theta neurons (hence we drop the population index σ) whose phases evolve according to

$$\dot{\theta}_k = 1 - \cos \theta_k + (1 + \cos \theta_k)(\eta_k + \kappa I), \quad (7)$$

³If there is only one population, $M = 1$, and we write $\alpha_{\sigma\tau} = \alpha$, $K_{\sigma\tau} = K$; this corresponds to the Kuramoto–Sakaguchi model. If further $\alpha = 0$ then we recover the Kuramoto model (3).

⁴Such form of interactions typically arise in an additional averaging step performed after the phase reduction [35, 67].

⁵The frequency ω_f of the co-rotating frame may depend on time; for example, for any given oscillator (σ, k) we may consider a co-rotating frame in which the phase $\theta_{\sigma,k}$ appears stationary.

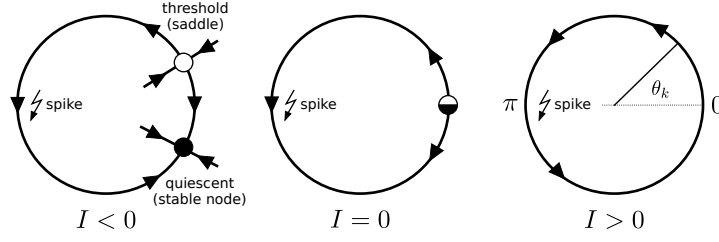


Fig 2. The Theta neuron model (7) displays a saddle node bifurcation on an invariant circle (SNIC).

where η_k is the excitability of oscillator k sampled from a probability distribution, I is an *input current*—this could result from external input (driving) or network interactions—and κ is the coupling strength. A population of Theta neurons (7) is a sinusoidally coupled system of the form (1) with

$$\omega_k = 1 + \eta_k + \kappa I, \quad H_k = i(\eta_k + \kappa I - 1). \quad (8)$$

The dependence of H, ω on the excitability parameters η_k can be made explicit by writing $\omega_k = \omega(\eta_k)$, $H(t) = H(t; \eta_k)$. Thus, results for models of the form (1) will also apply to networks of Theta neurons.

The Theta neuron [72] was introduced in 1986 and has since then been widely used in neuroscience. For example, [73] used these neurons as canonical type I neuronal oscillators in their study of chaotic dynamics in large, sparse balanced networks. The papers [74, 75] considered spatially extended networks of Theta neurons and the authors were specifically interested in traveling waves of activity in these networks. More recently other authors have used some of the techniques for dimension reduction reviewed in this paper to study infinite networks of Theta neurons [76, 77].

Quadratic Integrate and Fire neurons. The Theta neuron model is closely related to the Quadratic Integrate and Fire (QIF) neuron model [78, 79]. More precisely, using the transformation $V_k = \tan(\theta_k/2)$ the network (7) becomes a network of QIF neurons governed by

$$\dot{V}_k = V_k^2 + \eta_k + \kappa I \quad (9)$$

where V_k is the voltage of neuron k . Here we use the rule that the neuron fires if its voltage reaches $V_k(t^-) = \infty$ and then the neuron is reset to $V_k(t^+) = -\infty$.

QIF neurons have been widely used in neuroscientific modelling [78, 80–83]. They have the simplicity of the more common leaky integrate-and-fire (LIF) model in the sense of having only one state variable (the voltage) but are more realistic in the sense of actually producing an action potential, and (as mentioned) being related to the Theta neuron.

Exact mean-field descriptions for sinusoidally coupled phase oscillators

In this section, we review how sinusoidally coupled phase oscillator networks (1) can be simplified using mean-field reductions. Under specific assumptions (detailed further below) we derive low-dimensional system of ordinary differential equations for macroscopic mean-field variables

that describe the evolution of sinusoidally coupled phase oscillator networks (1) exactly. This is in contrast to reductions that are only approximate or only valid over short time scales. Thus, these reduction methods facilitate the analysis of the network dynamics: rather than looking at a complex, high-dimensional network dynamical system (or its infinite-dimensional continuum limit) we can analyze simpler, low-dimensional equations. For example, for the infinite-dimensional limit of the Kuramoto model, we obtain a closed system for the evolution of Z , a two-dimensional system (since Z is complex). While the Kuramoto model is particularly simple, the methods apply for general driving fields $H_{\sigma,k}$ that could contain delays or depend explicitly on time.

Importantly, these mean field reductions also apply to oscillator networks which are equivalent to (1). This applies in particular to neural oscillators: the QIF neuron and the Theta neuron are equivalent as discussed above. Consequently, rather than assuming a model for a neural population (e.g., [42]), we actually obtain an exact description of interacting neural populations in terms of their macroscopic (mean-field) variables.

Ott–Antonsen reduction for the continuum limit of nonidentical oscillators

The Ott–Antonsen reduction applies to the continuum limit of populations of indistinguishable sinusoidally coupled phase oscillators (1). We first outline the basic steps to derive the equations and highlight the assumptions made along the way; this section contains mathematical details and may be omitted on first reading. We then summarize the Ott–Antonsen equations for the models described in the previous section.

*Derivation of the reduced equations

We now consider the dynamics of (1) in the (continuum) limit of infinitely large networks, $N \rightarrow \infty$. To simplify the exposition, we consider the classical case that the intrinsic frequency is the random parameter, $\omega_{\sigma,k} = \eta_{\sigma,k}$, and that the driving field is the same for all oscillators in any population, $H_{\sigma,k} = H_{\sigma}$; for details on systems with explicit parameter dependence (such as Theta neurons) see [78, 84]. Hence, suppose that the intrinsic frequencies $\omega_{\sigma,k}$ are randomly drawn from a distribution with density $h_{\sigma}(\omega)$ on \mathbb{R} . In the continuum limit, the state of each population at time t is not given by a collection of oscillator phases, but rather by a probability density $f_{\sigma}(\omega, \vartheta; t)$ for an oscillator with intrinsic frequency $\omega \in \mathbb{R}$ to have phase $\vartheta \in \mathbb{T}$ at time t . For a set of phases $B \subset \mathbb{T}$ the marginal $\int_B \int_{\mathbb{R}} f_{\sigma}(\omega, \vartheta; t) d\omega d\vartheta$ determines the fraction of oscillators whose phase is in B at time t . Moreover, we have $\int_{\mathbb{T}} f_{\sigma}(\omega, \vartheta; t) d\vartheta = h_{\sigma}(\omega)$ for all times t by our assumption that the intrinsic frequencies do not change over time.

Conservation of oscillators implies that the dynamics of (1) in the continuum limit is given by the transport equation⁶

$$\frac{\partial f_{\sigma}}{\partial t} + \frac{\partial}{\partial \vartheta} (v_{\sigma} f_{\sigma}) = 0 \quad \text{with} \quad v_{\sigma} = \omega_{\sigma} + \text{Im}(H_{\sigma}(t)e^{-i\vartheta}). \quad (10)$$

Because oscillators are conserved⁷, the change of the phase distribution over time is determined by the change of phases given by the velocity v_{σ} through (1) at time t of an oscillator with phase ϑ

⁶If the oscillators are subject to noise, the continuity equation is a Fokker–Planck equation which contains an additional diffusive term [85–88].

⁷Transport equations are common in physics. There they are also known as the continuity equation (or Liouville equation in classical statistical physics describing the ensemble evolution in time) and play the important role of describing conservation laws. To visualize, in the context of fluid dynamics, the density in (10) plays the role of a mass density and (10) implies then that the total mass in the system is a conserved quantity [89].

and intrinsic frequency ω . While the transport equation for the continuum limit originally appears in Refs. [85,90], it can be derived in a mathematically rigorous way as a Vlasov-limit [91].

Before we discuss how to find solutions for the transport equation (10), it is worth noting that it has been analyzed directly in the context of functional analysis for networks of Kuramoto oscillators. Stationary solutions of (10) and their stability have been studied recently in the context of all-to-all coupled networks [92–95] and convergent families of random graphs [96]. (Roughly speaking, these are networks which have a well-defined limit as the number of nodes approaches infinity.)

Ott and Antonsen [97] showed that there exists a manifold of invariant probability densities for the transport equation (10). Specifically, if $f_\sigma(\vartheta, \omega, 0)$ satisfies the condition of the manifold, so will the density $f_\sigma(\vartheta, \omega, t)$ for any time $t \geq 0$. Let

$$Z_\sigma := \int_{-\infty}^{\infty} \int_{-\pi}^{\pi} f_\sigma(\vartheta, \omega, t) e^{-i\vartheta} d\vartheta d\omega \quad (11)$$

denote the Kuramoto order parameter (2) in the continuum limit. We will see below that the evolution on the invariant manifold is now described by a simple ordinary differential equation for Z_σ for each population σ .

In the following we outline the key steps to derive a set of reduced equations and refer to [97–99] for further details. Suppose that $f_\sigma(\vartheta, \omega, t)$ can be expanded into a Fourier series in the phase angle ϑ of the form

$$f_\sigma(\vartheta, \omega, t) = \frac{h_\sigma(\omega)}{2\pi} (1 + f_\sigma^+ + \bar{f}_\sigma^+) \quad \text{where} \quad f_\sigma^+ = \sum_{n=1}^{\infty} f_\sigma^{(n)}(\omega, t) e^{in\vartheta}. \quad (12)$$

Here it is assumed that f_σ^+ has an analytic continuation into the complex half plane $\{\text{Im}(\vartheta) > 0\}$ (and $f_\sigma^- := \bar{f}_\sigma^+$ into $\{\text{Im}(\vartheta) < 0\}$); even with this assumption we can solve a large class of problems, but it poses a restriction to a number of practical cases discussed in the section [*Limitations and challenges](#) below. Ott and Antonsen now imposed the ansatz that Fourier coefficients are powers of a single function $a_\sigma(\omega, t)$,

$$f_\sigma^{(n)}(\omega, t) = [a_\sigma(\omega, t)]^n. \quad (13)$$

If $|a_\sigma(\omega, t)| < 1$ this ansatz is equivalent to the Poisson kernel structure for the unit disk, $f_\sigma^+ = (a_\sigma e^{i\vartheta}) / (1 - a_\sigma e^{i\vartheta})$. Substitution of (12) into (10) yields

$$\frac{\partial a_\sigma}{\partial t} + i\omega a_\sigma + \frac{1}{2}(H_\sigma a_\sigma^2 - \bar{H}_\sigma) = 0, \quad (14)$$

Thus, the ansatz (13) reduces the integral partial differential equation (10) to a single ordinary differential equation⁸ in a_σ for each population σ . Finally, with (13) we obtain

$$Z_\sigma = \int_{-\infty}^{\infty} h_\sigma(\omega) a_\sigma(\omega, t) d\omega, \quad (15)$$

which relates a_σ and the order parameter Z_σ in (11). Assuming analyticity, this integral can sometimes be evaluated using the residue theorem of complex analysis.

These equations take a particularly simple form if the distribution of intrinsic frequencies $h_\sigma(\omega)$ is Lorentzian with mean $\hat{\omega}_\sigma$ and width Δ_σ , i.e.,

$$h_\sigma(\omega) = \frac{1}{\pi} \frac{\Delta_\sigma}{(\omega - \hat{\omega}_\sigma)^2 + \Delta_\sigma^2}, \quad (16)$$

⁸To be precise, there is an infinite set of such equations, for each ω , with identical structure.

since $h_\sigma(\omega)$ has poles at $\hat{\omega}_\sigma \pm i\Delta_\sigma$ and thus (15) gives $Z_\sigma = a_\sigma(\hat{\omega}_\sigma - i\Delta_\sigma, t)$. As a result, we obtain the two-dimensional differential equation—the **Ott–Antonsen equations** for a Lorentzian frequency distribution—for the order parameter in population σ ,

$$\dot{Z}_\sigma = -(\Delta_\sigma + i\hat{\omega}_\sigma)Z_\sigma + \frac{1}{2}H_\sigma - \frac{1}{2}\bar{H}_\sigma Z_\sigma^2. \quad (\text{OA})$$

We note that this reduction method also works for other frequency distribution h_σ as outlined in [99]. However, the resulting mean field equation will not always be a single equation but could be a set of coupled equations. For example, for multi-modal frequency distributions h_σ the Ott–Antonsen equations will have an equation for each mode; see [84, 100, 101] and the discussion below.

The derivation above only states that there *is* an invariant manifold of densities f_σ for the transport equation (10). What happens to densities f_σ that are not on the manifold as time evolves? Under some assumptions on the distribution in intrinsic frequencies h_σ , Ott and Antonsen also showed in [98] that there are densities f_σ that are attracted to the invariant manifold. In other words, the dynamics of the Ott–Antonsen equations capture the long-term dynamics of a wider range of initial phase distributions $f_\sigma(\vartheta, \omega, 0)$, whether they satisfy (13) initially or not.

Ott–Antonsen equations for commonly used oscillator models

We now summarize the Ott–Antonsen equations (OA) for the commonly used oscillator models described in the section [Sinusoidally coupled phase oscillator networks](#). Here we focus on Lorentzian distributions of the intrinsic frequencies or excitabilities; for Ott–Antonsen equations for other parameter distributions such as Normal or bimodal distributions see [97, 100].

Kuramoto Model. Consider the continuum limit of the Kuramoto model (3) with a Lorentzian distribution of intrinsic frequencies. Recall that the driving field for the Kuramoto model was $H(t) = KZ(t)$. Substituting this into (OA) we obtain *Ott–Antonsen equations for the Kuramoto model*

$$\dot{Z} = -(\Delta + i\hat{\omega})Z + \frac{K}{2}Z - \frac{K}{2}|Z|^2 Z, \quad (17)$$

a two-dimensional system of equations since Z is complex-valued.

Kuramoto–Sakaguchi equations. For the Kuramoto–Sakaguchi equations (4) the driving field is a weighted sum of the individual population order parameters (6). Assuming a Lorentzian distribution of intrinsic frequencies with mean $\hat{\omega}_\sigma$ and width Δ_σ for each population, from (OA) we obtain *Ott–Antonsen equations for coupled populations of Kuramoto–Sakaguchi oscillators*

$$\dot{Z}_\sigma = -(\Delta_\sigma + i\hat{\omega}_\sigma)Z_\sigma + \frac{1}{2} \left(\sum_{\tau=1}^M c_{\sigma\tau} Z_\tau - Z_\sigma^2 \sum_{\tau=1}^M \bar{c}_{\sigma\tau} \bar{Z}_\tau \right) \quad (18)$$

for populations $\sigma = 1, \dots, M$. In other words, the Ott–Antonsen equations are a $2M$ -dimensional system that describe the interactions of the order parameters Z_σ .

Networks of Theta neurons. Consider a single population of Theta neurons with drive $I(t)$ given by (7) with parameter-dependent intrinsic frequencies and driving field (8); we omit the population index σ . Assume that the variations in excitability η_k are chosen from a Lorentzian

distribution mean $\hat{\eta}$ and width Δ . We obtain the *Ott–Antonsen equations for the continuum limit of a population of Theta neurons* (8)

$$\dot{Z} = \frac{1}{2} ((i\hat{\eta} - \Delta)(1 + Z)^2 - i(1 - Z)^2) + \frac{1}{2} i(1 + Z)^2 \kappa I. \quad (19)$$

Note that in contrast to (18), this is not a closed set of equations yet as the exact form of the input current is still unspecified. We will close these equations in section [Populations of Theta neurons](#) below by writing I in terms of Z for different types of neural interactions.

The order parameter for the Theta neuron directly relates to quantities with a physical interpretation such as the average firing rate of the network. Integrating the phase distribution (12) over the excitability parameter η under assumption (13) we obtain the distribution of all phases,

$$p(\theta, t) = \frac{1}{2\pi} \left(\frac{1 - |Z|^2}{1 - Ze^{-i\theta} - \bar{Z}e^{i\theta} + |Z|^2} \right) = \frac{1}{2\pi} \operatorname{Re} \left(\frac{1 + \bar{Z}e^{i\theta}}{1 - \bar{Z}e^{i\theta}} \right), \quad (20)$$

where Z may be a function of time. This distribution can be used to determine the probability that a Theta neuron has phase θ . Since a Theta neuron fires when its phase crosses $\theta = \pi$, the average firing rate r of the network at time t is the flux through $\theta = \pi$, i.e.,

$$r = (p(\theta, t)\dot{\theta})|_{\theta=\pi} = \frac{1}{\pi} \operatorname{Re} \left(\frac{1 - \bar{Z}(t)}{1 + \bar{Z}(t)} \right). \quad (21)$$

Here we used that $\dot{\theta}|_{\theta=\pi} = 2$ by (7), independent of θ .

Ott–Antonsen reduction for equivalent networks

The mean field reductions are also valid for systems that are *equivalent* to a network of sinusoidally coupled phase oscillators (1). As an example, we discussed the relationship between QIF and Theta neurons above.

This transformation now carries over to the continuum limit of infinitely many neurons where the Ott–Antonsen equations apply. More specifically, the transformation $V = \tan(\theta/2)$ converts the distribution of phases (20) into a distribution

$$\tilde{p}(V, t) = \frac{X(t)}{\pi((V - Y(t))^2 + X^2(t))} \quad (22)$$

of voltages where $Z = (1 + \bar{W})/(1 - \bar{W})$ and $W = X + iY$ and $X, Y \in \mathbb{R}$. Equation (22) is called the *Lorentzian ansatz* in [78]. Importantly, the quantity W is obtained from a conformal transformation of the order parameter Z . This allows one to convert the Ott–Antonsen equations for the Theta neurons (19) to an equation for the mean field $W = (1 - \bar{Z})/(1 + \bar{Z})$,

$$\dot{W} = i\hat{\eta} + \Delta - iW^2 + iI, \quad (23)$$

which describes the QIF neurons. The advantage of this formulation is that both the real and imaginary parts of W have physical interpretations: $Y(t)$ is the average voltage across the network and $X(t)$ relates to the firing rate r of the population, i.e., the flux at $V = \infty$, since $\lim_{V \rightarrow \infty} \tilde{p}(V, t)\dot{V}(t) = X(t)/\pi = r$ [78].

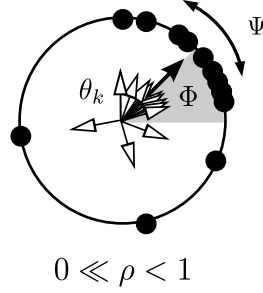


Fig 3. Illustration of the bunch variables in the Watanabe–Strogatz formalism. Just like the Kuramoto order parameter Z_σ , the bunch amplitude and bunch phase in $z_\sigma = \rho_\sigma e^{i\Phi_\sigma}$ characterize the level of synchrony. The quantities Z_σ and z_σ do however only coincide if the population is fully synchronized or for uniformly distributed constants of motion in the limit $N \rightarrow \infty$ (see text). The phase distribution variable Ψ_σ is related to the shift and distribution of individual oscillators with respect to Φ_σ .

Watanabe–Strogatz reduction for identical oscillators

Mean-field reductions are possible for both finite and infinite networks for populations of identical oscillators. These reductions are due to the high level of degeneracy in the system, i.e., there are many quantities that are conserved as time evolves. This degeneracy was first observed in the early 1990s for coupled Josephson junction arrays [102], which relate directly to Kuramoto’s model of coupled phase oscillators [103]. Watanabe and Strogatz [104, 105] were able to calculate the preserved quantities explicitly using a clever transformation of the phase variables, thereby reducing the Kuramoto model from N (oscillator phases) to three time-dependent (mean-field) variables together with $N - 3$ constants of motion. In terms of mathematical theory, the degeneracy originates from a rich algebraic structure of the equations [106–108] which is still an area of active research [109].

The Watanabe–Strogatz reduction applies for sinusoidally coupled phase oscillator populations where oscillators within populations are identical, i.e., all oscillators have the same intrinsic frequency, $\omega_{\sigma,k} = \omega_\sigma$, and are driven by the same field $H_{\sigma,k} = H_\sigma$. Indeed, Watanabe–Strogatz and Ott–Antonsen reductions have been shown to be intricately linked [107, 110] as we briefly discuss below. Here, we focus on finite networks for simplicity. In the following section we give the equations in generality and give some mathematical detail. Then, the equations are subsequently stated for the commonly used oscillator models discussed above.

*Constants of motion yield reduced equations

The dynamics of a finite population (1) with $N > 3$ identical oscillators can be described exactly in terms of three macroscopic (mean-field) variables [104, 105, 110, 111]: the bunch amplitude ρ_σ , bunch phase Φ_σ , and phase distribution variable Ψ_σ . Similar to the Kuramoto order parameter Z_σ , the bunch amplitude ρ_σ and bunch phase Φ_σ characterize synchrony (or equivalently, the maximum of the phase distribution); while Z_σ and $(\rho_\sigma, \Phi_\sigma)$ do not coincide in general, they do if the population is fully synchronized. The phase distribution variable Ψ_σ determines the shift of individual oscillators with respect to Φ_σ as illustrated in Fig. 3.

For a population of sinusoidally coupled phase oscillators (1) with driving field $H_\sigma = H_\sigma(t)$

the macroscopic variables evolve according to the **Watanabe–Strogatz equations**

$$\dot{\rho}_\sigma = \frac{1 - \rho_\sigma^2}{2} \operatorname{Re}(H_\sigma e^{-i\Phi_\sigma}), \quad (\text{WSa})$$

$$\dot{\Phi}_\sigma = \omega_\sigma + \frac{1 + \rho_\sigma^2}{2\rho_\sigma} \operatorname{Im}(H_\sigma e^{-i\Phi_\sigma}), \quad (\text{WSb})$$

$$\dot{\Psi}_\sigma = \frac{1 - \rho_\sigma^2}{2\rho_\sigma} \operatorname{Im}(H_\sigma e^{-i\Phi_\sigma}). \quad (\text{WSc})$$

Mathematically speaking, the reduction to three variables means that the phase space \mathbb{T}^N of (1) is foliated by 3-dimensional leafs, each of which is determined by constants of motion, $\psi_k^{(\sigma)}$, $k = 1, \dots, N$ ($N - 3$ are independent). In other words, the choice of constants of motion determines a specific 3-dimensional invariant subspace on which the macroscopic variables evolve. The Watanabe–Strogatz equations arise from the properties of Riccati equations and the bunch variables are parameters of a family of Möbius transformations which determine the system's dynamics; see [107–109] for more details on the mathematics behind these equations.

From a practical point of view, two things are needed to use the Watanabe–Strogatz equations (WS) to understand oscillator networks of the form (1). First, since the driving field H is often a function of the population order parameters Z_τ , $\tau = 1, \dots, M$, we need to translate Z_σ into the bunch variables to get a closed set of equations. Write $z_\sigma := \rho_\sigma e^{i\Phi_\sigma}$. As shown for example in [110], we have

$$Z_\sigma = z_\sigma \gamma_\sigma \quad \text{where} \quad \gamma_\sigma = \frac{1}{N\rho_\sigma} \sum_{j=1}^N \frac{\rho_\sigma e^{i\Psi_\sigma} + e^{i\psi_j^{(\sigma)}}}{e^{i\Psi_\sigma} + \rho_\sigma e^{i\psi_j^{(\sigma)}}}. \quad (25)$$

Second, one needs to determine the constants of motion from the initial phases $\theta_{\sigma,k}(0)$; this is discussed in detail in [105], but a possible choice is to set $\psi_k^{(\sigma)} := \theta_{\sigma,k}(0)$ and $\rho_\sigma(0) = \Phi_\sigma(0) = \Psi_\sigma(0) = 0$. Taken together, the dynamics of individual oscillators (1) are now determined by (WS) via (25) and vice versa.

The relationship (25) between the bunch variables and the order parameter also indicates how the Watanabe–Strogatz equations and the Ott–Antonsen equations are linked. Pikovsky and Rosenblum [111] showed that for constants of motion that are uniformly distributed on the circle, $\psi_k^{(\sigma)} = 2\pi k/N$, we have $\gamma_\sigma \rightarrow 1$ as $N \rightarrow \infty$. In this case, the bunch variable z_σ is identical to the Kuramoto order parameter in the limit. Moreover, the equation (WSc) decouples from equations (WSa) and (WSb), which are equivalent to the Ott–Antonsen equations (OA) in the continuum limit. To summarize, the dynamics of the continuum limit for identical oscillators is given by the Watanabe–Strogatz equations together with a *distribution* of constants of motion. For the particular choice of a uniform distribution of constants of motion, the equations decouple and the effective dynamics are given by the Ott–Antonsen equations.

Watanabe–Strogatz equations for commonly used oscillator models

We now summarize the Watanabe–Strogatz equations (WS) for the commonly used oscillator models described in the section [Sinusoidally coupled phase oscillator networks](#).

Kuramoto–Sakaguchi equations. For the multi-population Kuramoto–Sakaguchi model (4), the driving field H is a linear combination of the order parameters, $H_\sigma := \sum_{\tau=1}^M c_{\sigma\tau} Z_\tau$. Assuming that the oscillators within each population are identical, $\omega_{\sigma,k} = \omega_\sigma$, the dynamics are

governed by the *Watanabe–Strogatz equations for coupled Kuramoto–Sakaguchi populations*

$$\dot{\rho}_\sigma = \frac{1 - \rho_\sigma^2}{2} \operatorname{Re} \left(\sum_{\tau=1}^M c_{\sigma\tau} \gamma_\tau \rho_\tau e^{i(\Phi_\tau - \Phi_\sigma)} \right), \quad (26a)$$

$$\dot{\Phi}_\sigma = \omega_\sigma + \frac{1 + \rho_\sigma^2}{2\rho_\sigma} \operatorname{Im} \left(\sum_{\tau=1}^M c_{\sigma\tau} \gamma_\tau \rho_\tau e^{i(\Phi_\tau - \Phi_\sigma)} \right), \quad (26b)$$

$$\dot{\Psi}_\sigma = \frac{1 - \rho_\sigma^2}{2\rho_\sigma} \operatorname{Im} \left(\sum_{\tau=1}^M c_{\sigma\tau} \gamma_\tau \rho_\tau e^{i(\Phi_\tau - \Phi_\sigma)} \right). \quad (26c)$$

Networks of Theta neurons. For a finite population of identical Theta neurons (8) with identical excitability η and input current $I(t)$ the *Watanabe–Strogatz equations for identical Theta neurons* [112] evaluate to

$$\dot{\rho} = \frac{1 - \rho^2}{2} \operatorname{Re} (i(\eta + I - 1)e^{-i\Phi}), \quad (27a)$$

$$\dot{\Phi} = 1 + \eta + I + \frac{1 + \rho^2}{2\rho} \operatorname{Im} (i(\eta + I - 1)e^{-i\Phi}), \quad (27b)$$

$$\dot{\Psi} = \frac{1 - \rho^2}{2\rho} \operatorname{Im} (i(\eta + I - 1)e^{-i\Phi}). \quad (27c)$$

Note that, as for the Ott–Antonsen reduction above, one still needs to close this system by writing I in terms of the bunch variables in (WS) and the constants of motion. This is not straightforward and requires a considerable amount of computations [112].

Reductions for equivalent networks

For a finite network of identical QIF neurons governed by (9) with $\eta_j = \eta$ for all j , the transformation $V = \tan(\theta/2)$ converts this network into a network of identical Theta neurons (7). Consequently, such a network will also be described by equations of the form (27). As mentioned above, in the limit $N \rightarrow \infty$ and equally spaced constants of motion, the equation (27c) will decouple from (27a) and (27b). In this case, writing $z = \rho e^{i\Phi}$ we find that z satisfies (19) or equivalently (23) (with $\hat{\eta} = \eta$ and $\Delta = 0$).

*Limitations and challenges

Before we apply the mean field reductions to particular oscillator networks in the next section, some (mathematical) comments on the limitations of these approaches are in order; this section may be skipped at first reading.

As stated above, the main assumption is that of interactions through a sinusoidal coupling function. There are explicit examples [88, 113, 114] that show that the reductions, as described above, become invalid. For example chaotic dynamics may occur where the reduction would have an effective two-dimensional phase space; we discuss this example below. This does not mean that the reductions break down completely, and there may still be some degeneracy in the system if the interaction is of a specific form; see [115] for a more detailed discussion. It remains a challenge to identify what part of the mean-field reduction (if any) remains valid for more general interaction functions and phase response curves.

The Ott–Antonsen reduction for the continuum limit allows for the oscillators to be nonidentical. By contrast, the Watanabe–Strogatz reduction of finite networks requires oscillators to be

identical. Neither of these approaches applies to finite networks of nonidentical oscillators, and understanding such networks remains a challenge. There has also been some recent progress analyzing situations in which the Ott–Antonsen or Watanabe–Strogatz equations do not apply, using perturbation theory [116]. Note that direct numerical simulations for networks of N almost identical oscillators poses a challenge as one needs to integrate an almost integrable dynamical system.

Finally, Ott and Antonsen showed that the manifold of oscillator densities f_σ on which the reduction holds is attracting [98]. Their method of proof has been shown to apply to a wider class of systems [84]. As pointed out by Mirollo [117], their proof is based on a strong smoothness assumption on the density f_σ which implies limitations to this approach. More precisely, to be able to evaluate contour integrals using the residue theorem, it is typically assumed that the density is holomorphic. This assumption is only valid for distributions h_σ that allow for arbitrarily large (or small) intrinsic frequencies with nonzero probability: the identity theorem for holomorphic functions implies that $h_\sigma(\omega) > 0$ for all $\omega \in \mathbb{R}$. Any distribution for which the intrinsic frequencies are bound to a finite interval—the intrinsic frequencies of any finite collection of oscillators will lie in a finite interval—are excluded. Hence, while the manifold described by Ott and Antonsen attracts some class of oscillator densities (which include some commonly used ones like Lorentzians and Gaussians), it is not clear how large this class actually is.

Dynamics of coupled oscillator networks

We now discuss global synchrony and synchrony patterns in phase oscillator networks that are of relevance from the point of view of biology and neuroscience. In particular, for sinusoidally coupled networks, we will highlight how the reductions presented in the previous section simplify analyses.

Networks of identical populations of Kuramoto–Sakaguchi oscillators

First we discuss identical (and almost identical) populations of Kuramoto–Sakaguchi oscillators (4) with Lorentzian distribution of intrinsic frequencies; results for nonidentical populations are given later. To be precise, we say that all populations of (4) are *identical* if for any two populations σ, τ , there is a permutation which sends σ to τ and leaves the corresponding equations (18) for the continuum limit invariant. Intuitively speaking, this means we can swap any population with any other population without changing the dynamics. Mathematically speaking, the populations are identical if the Ott–Antonsen equations (18) have a permutational symmetry group that acts transitively [118]. If the populations are identical, then the frequency distributions h_σ are the same for all populations. Moreover, if the oscillators within each population have the same intrinsic frequency (as required for the Watanabe–Strogatz reduction) then all oscillators in the network have the same intrinsic frequency.

Oscillator networks which are organized into populations support *synchrony patterns* which may be *localized*, that is, some populations show more (or less) synchrony than others. While this may not be surprising if the populations are nonidentical, such dynamics may also occur when the populations are identical. For identical populations, the localized dynamics arise purely through the network interactions—the populations would behave identically if uncoupled—and hence constitute a form of dynamical symmetry breaking. This effect has been dubbed a *chimera state* in the literature and has attracted a tremendous amount of attention in the last two decades; see [49–51] for recent reviews. While an entire zoo of chimeras and chimera-like creatures has emerged in a range of networked dynamical systems—with the appropriate attempts to classify

and distinguish these creatures [119, 120]—we will discuss chimeras here in (4), the (original) context of localized (phase and frequency) synchrony of phase oscillators [121].

One oscillator population

We first consider Kuramoto’s original problem [64] about the onset of synchronization in the globally coupled network (3) that was outlined in the section [The Kuramoto model](#) above: For what coupling strength K do nonidentical Kuramoto oscillators start to synchronize? This problem is surprisingly easy to solve in the continuum limit $N \rightarrow \infty$ using the Ott–Antonsen reduction. Assume that the distribution of intrinsic frequencies is a Lorentzian with width Δ and mean $\hat{\omega}$. Recall that the order parameter Z evolves according to the Ott–Antonsen equation (17): separating (17) into real and imaginary parts yields an equation for $R = |Z|$, given by

$$\dot{R} = \left(-\Delta + \frac{K}{2} - \frac{K}{2} R^2 \right) R, \quad (28)$$

and an equation for the mean phase ϕ which is driven by R . Moreover, the manifold on which (28) describes the continuum limit of (3) attracts all initial phase distributions. Thus, Kuramoto’s problem in the infinite-dimensional continuum limit reduces to solving the one-dimensional real ordinary differential equation (17): by elementary analysis, we find that the equilibrium $R = 0$ is stable for $K < K_c = 2\Delta$ and loses stability in a pitchfork bifurcation where the solution $R = \sqrt{1 - 2\Delta/K} > 0$ becomes stable. The same analysis applies to the Kuramoto–Sakaguchi network (4) with $M = 1$ for phase-lag $\alpha \in (-\frac{\pi}{2}, \frac{\pi}{2})$ with K replaced by $K \cos(\alpha)$.

Global synchronization of finite networks of identical Kuramoto–Sakaguchi oscillators is readily analyzed using the Watanabe–Strogatz reduction. As above, a phase variable decouples and we obtain a two-dimensional system which describes the dynamics of (4) for $M = 1$. Its analysis [104] shows that the system will synchronize perfectly, $R \rightarrow 1$ as $t \rightarrow \infty$, for $\alpha \in (-\frac{\pi}{2}, \frac{\pi}{2})$ (attractive coupling) and converge to an incoherent equilibrium, $R \rightarrow 0$ as $t \rightarrow \infty$, for $\alpha \in (\frac{\pi}{2}, \frac{3\pi}{2})$ (repulsive coupling).

Much progress has been made to understand synchronization and more complicated collective dynamics in globally coupled networks of Kuramoto oscillators and their generalizations; see [87, 122, 123] for surveys. While we discussed Kuramoto’s problem as an example, the same methods apply for more general types of driving fields H : they may include delays [97], be heterogeneous in terms of the contribution of individual oscillators [124], or generalized mean fields [109]. However, note that much richer dynamics are possible when the assumptions of sinusoidal coupling breaks down. Because of the Poincaré–Bendixson theorem [125], chaos is not possible for the mean field reductions for $M = 1$ populations of Kuramoto–Sakaguchi oscillators since their effective dynamics is one- or two-dimensional, respectively. By contrast, even for fully symmetric networks, higher harmonics in the phase response curve/coupling function may lead to chaotic dynamics [113, 114].

Two oscillator populations

The Ott–Antonsen reduction is also instrumental to understand the dynamics of networks consisting of $M = 2$ populations of Kuramoto–Sakaguchi oscillators. Assuming that all intrinsic frequencies are distributed according to a Lorentzian, we obtain two coupled Ott–Antonsen equations (18) for the limit of infinitely large populations. In this section we focus on networks of identical populations, that is, the distributions of intrinsic frequencies are the same and coupling

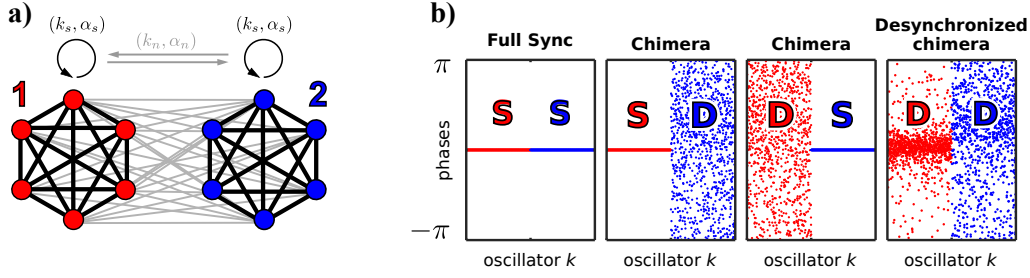


Fig 4. Synchronization patterns for a network with $M = 2$ populations (red and blue) by simulation of Eqs. (4) with $N = 1000$ oscillators per population parameters $A = 0.7, \alpha_n = 0.44$ and $\alpha_s = 1.58, 1.58, 1.58, 1.64$ (from left to right).

is symmetric; cf. Fig. 4(a). This allows to simplify the parametrization of the system by introducing *self-coupling* $c_s = k_s e^{-i\alpha_s} := c_{11} = c_{22}$ and *neighbor-coupling* $c_n = k_n e^{-i\alpha_n} := c_{12} = c_{21}$ parameters and the coupling strength disparity $A = (k_s - k_n)/(k_s + k_n)$. Writing $Z_\sigma = R_\sigma e^{i\phi_\sigma}$ as above, the state of (18) is fully determined by the amount of synchrony in each population R_1, R_2 and the difference of the mean phase $\psi := \phi_1 - \phi_2$ of the two populations; cf. [126]. Naturally, such networks support three *homogeneous synchronized states*, a fully synchronized state $SS_0 = \{(R_1, R_2, \psi) = (1, 1, 0)\}$ where both populations are synchronized and in phase, a cluster state $SS_\pi = \{(R_1, R_2, \psi) = (1, 1, \pi)\}$ where both populations are synchronized, and in anti-phase and a completely incoherent state $I = \{(R_1, R_2, \psi) = (0, 0, *)\}$. A bifurcation analysis shows that only one of the three is stable for any given choice of coupling parameters [126].

In addition to homogeneous synchronized states, networks of two populations also support chimeras where synchrony is localized in one of the two populations as illustrated in Fig. 4(b). Abrams *et al.* [127] found that for *homogeneous phase-lags*, $\alpha_s = \alpha_n$, stable synchrony SS_0 coexists with a stable chimera in $DS = \{R_1 < 1, R_2 = 1\}$ which is either stationary or oscillatory⁹. Note that the Ott–Antonsen reduction simplifies the analysis tremendously: it translates the problem for large oscillator networks into a low-dimensional bifurcation problem. Martens *et al.* [128] outlined the basins of attraction of the coexisting stable synchrony patterns and thereby answering the question as to which (macroscopic or microscopic) initial conditions converge to either state. Further work addresses the robustness of chimera states against various inhomogeneities, including heterogeneous frequencies [129, 130], network heterogeneity [131], and additive noise [130].

If one allows for *heterogeneous phase-lag parameters*, $\alpha_s \neq \alpha_n$, a variety of other attractors with localized synchrony emerge [126, 132]. This includes in particular solutions in $DD = \{R_1, R_2 < 1\}$ where neither population is fully phase synchronized; cf. Fig. 4(b). This includes not only stationary or oscillatory solutions of the state variables, but also attractors where the order parameters Z_1, Z_2 fluctuate chaotically both in amplitude and with respect to their phase difference [133].

Finite networks with two populations of identical oscillators may be analyzed using the Watanabe–Strogatz equations (26). One finds that the bifurcation scenarios for the appearance of chimera states is similar to the dynamics observed for infinite populations [134]. Moreover, macroscopic chaos also appears in many finite networks [133] down to just two oscillators per population.

⁹By symmetry there is a corresponding pattern in $SD = \{R_1 = 1, R_2 < 1\}$.

Localized frequency synchrony in small oscillator networks. For finite oscillator networks, the widely used intuitive definition of a chimera as a solution for networks of (almost) identical oscillators where “coherence and incoherence coexist” is difficult to apply in a mathematically rigorous way. Hence, Ashwin and Burylko [135] introduced the concept of a *weak chimera* which provides a mathematically testable definition of a chimera state in finite networks of identical oscillators; here, we only give an intuition and refer to [135, 136] for a precise definition. The main feature of a weak chimera is that identical oscillatory units (with the same intrinsic frequency if uncoupled) generate rhythms with two or more distinct frequencies solely through the network interactions. In the context of dynamical systems with symmetry [118], weak chimeras are—as outlined in [137]—an example of dynamical symmetry breaking where identical elements have nonidentical dynamics since their frequencies are distinct.

More specifically, a weak chimera is characterized by localized frequency synchrony in a network of identical oscillators. Similar to the definition of identical populations above, we say that the oscillators are identical if for a pair of oscillators (σ, k) and (τ, j) there exists an invertible transformation of the oscillator indices which keeps the equations of motion invariant. In other words, all oscillators are effectively equivalent. Now $\dot{\theta}_{\sigma,k}(t)$ is the *instantaneous frequency* of oscillator (σ, k) —the change of phase at time t —and thus the *asymptotic average frequency* of oscillators (σ, k) is

$$\Omega_{\sigma,k} = \lim_{T \rightarrow \infty} \frac{1}{T} \int_0^T \dot{\theta}_{\sigma,k}(t) dt. \quad (29)$$

Rather than looking at phase synchrony ($\theta_{\sigma,k} = \theta_{\tau,j}$) of oscillators (σ, k) and (τ, j) , we say that the oscillators are *frequency synchronized* if $\Omega_{\sigma,k} = \Omega_{\tau,j}$. Weak chimeras now show *localized frequency synchrony*, that is, all oscillators within one population have the same frequency $\Omega_\sigma = \Omega_{\sigma,k}$ while there are at least two distinct populations τ, τ' that have different frequencies, $\Omega_\tau \neq \Omega_{\tau'}$. Note that weak chimeras are impossible for a globally coupled network of identical phase oscillators (that is, there is only a single population $M = 1$): Such a network structure forces frequency synchrony of all oscillators [135].

Weak chimeras have been shown to exist in a range of networks which consist of $M = 2$ interacting populations of phase oscillators. For weakly interacting populations of phase oscillators with general interaction functions there can be stable weak chimeras with quasiperiodic [135, 138] and chaotic dynamics [136]. However, neither weak interaction nor general coupling functions are necessary for dynamics with localized frequency to arise: even sinusoidally coupled networks (4) of just $N = 2$ oscillators per population support stable regular [134] and chaotic [133] weak chimeras.

Three and more oscillator populations

Chimeras as patterns of localized synchrony arise naturally in networks of $M = 3$ populations of Kuramoto–Sakaguchi oscillators (4). In the first part of this section, we focus on the mean field dynamics for infinitely many oscillators where the Ott–Antonsen reduction applies. These networks give rise to a range of synchronization patterns. Since networks consisting of $M = 3$ populations have received relatively little attention, we restrict ourselves to the cases treated in [139, 140] where populations are identical and symmetrically coupled, $c_{\sigma\tau} = c_{\tau\sigma}$. Then the coupling is determined by self-coupling k_s and phase-lag α_s , as well as coupling strength and phase lag to the neighboring populations k_{n_1}, k_{n_2} and $\alpha_{n_1}, \alpha_{n_2}$; cf. Fig. 5(a). Reducing the phase-shift symmetry, we have that the state of the system is determined by the magnitude of the order parameters, $R_\sigma = |Z_\sigma|$ and the phase differences between the mean fields $\psi_1 = \phi_2 - \phi_1$ and $\psi_2 = \phi_3 - \phi_1$.

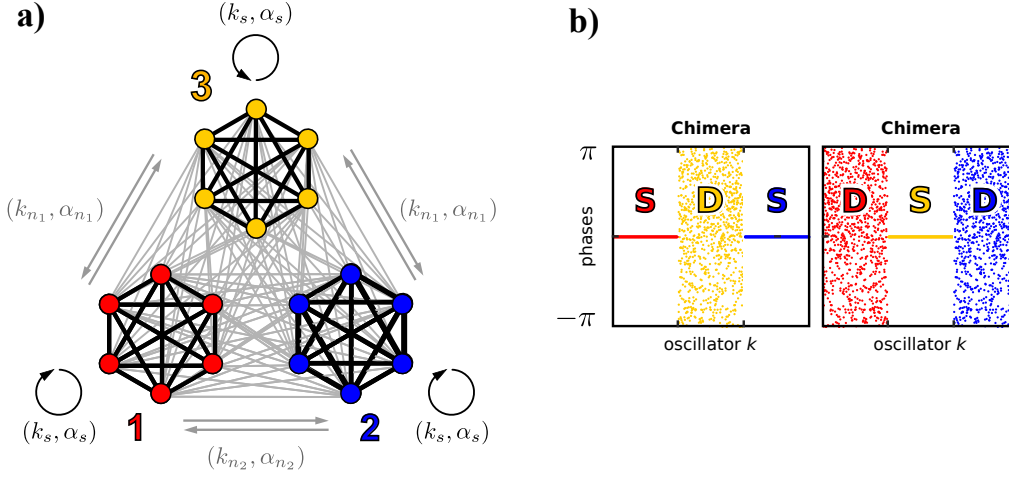


Fig 5. Sketch of synchronization patterns for chimera states (b) for a finite approximation of networks of $M = 3$ populations (b) with symmetric self- and neighbor interaction parameters, $(k_s, k_{n1,2}, \alpha_s, \alpha_{n1,2})$, as described in the main text.

Networks of three populations support a variety of localized synchrony patterns; cf. Fig. 5(b). In [139], Martens considers coupling with a triangular symmetry, that is, $k_{n1} = k_{n2} \leq k_s$ and $\alpha_{n1} = \alpha_{n2}$. There are three stable solution branches, full phase synchrony $\text{SSS} = \{R_1 = R_2 = R_3 = 1\}$ as well as two chimeras in $\text{SDS} = \{R_1 = R_3 = 1 > R_2\}$ and in $\text{DSD} = \{R_1 = R_3 < R_2 = 1\}$. The Ott–Antonsen reduction allows one to perform an explicit bifurcation analysis of the resulting planar system and shows bifurcations similar to networks with $M = 2$ populations. Remarkably, there are parameter values where SSS as well as the chimeras in SDS, DSD are stable simultaneously; this gives rise to the possibility of switching between these three synchronization patterns through directed perturbations [128]. This triangular symmetry is broken in [140] by allowing $k_{n2} \neq k_{n1}$. Thus, the coupling between populations 2 and 3 can be gradually reduced or increased until the network effectively becomes a chain of three populations or effectively two populations, respectively. A bifurcation analysis shows that the chimeras in SDS and DSD persist and provides stability boundaries.

Metastability and dynamics of localized synchrony. The synchrony patterns above were primarily considered as attractors: for a range of initial phase configurations, the long term dynamics of the oscillator network will exhibit a particular synchrony pattern. While this may be a good approximation for large scale neural dynamics on a short time-scale, the global dynamics of large-scale brain neural networks are usually much more complicated [23]. Neural recordings show that particular dynamical states (of synchrony and activity) persist for some time before a rapid transition to another state [46, 141, 142]. One approach to model such dynamics is to assume that there are a number of *metastable states* (rather than attractors) in the network phase space which are connected dynamically by *heteroclinic trajectories*¹⁰ [143]. If heteroclinic trajectories form a *heteroclinic network*¹¹—the nodes of this network are dynamical states, links

¹⁰A heteroclinic trajectory between two distinct saddles is a solution that is attracted to one saddle as time increases and to the other saddle as time evolves backward.

¹¹Unfortunately, the term “network” has a double meaning here: on the one hand, we study oscillatory units which form networks through their (physical and functional) interactions, on the other hand, heteroclinic networks are abstract

are connecting heteroclinic trajectories—the system can exhibit sequential switching dynamics: the state will stay close to one metastable state before a rapid transition, or switch, to the next dynamical state. Heteroclinic networks have long been subject to investigations, both theoretically [144] and with respect to applications in neuroscience [35]; one possible modeling approach is to write down kinetic (Lotka–Volterra type) equations for interacting macroscopic activity patterns [145, 146] which support heteroclinic networks.

Heteroclinic dynamics also arise in phase oscillator networks. For globally coupled oscillator networks, i.e., $M = 1$ population, there are heteroclinic networks between patterns of phase synchrony [147, 148]. As mentioned above, all oscillators in these networks are necessarily frequency synchronized, that is, they show the same rate of activity. More recently, it was shown that more general network interactions than those in (4) allow for *heteroclinic switching between weak chimeras* as states with localized frequency synchrony [149]: each population will sequentially switch between states with high activity (frequency) to a state with low activity. One of the simplest phase oscillator networks which exhibits such dynamics consists of $M = 3$ populations of $N = 2$ oscillators where $K > 0$ mediates the coupling strength between populations. More precisely, the dynamics of oscillator (σ, k) are given by

$$\begin{aligned}\dot{\theta}_{\sigma,k} = & \sin(\theta_{\sigma,3-k} - \theta_{\sigma,k} + \alpha) + r \sin(2(\theta_{\sigma,3-k} - \theta_{\sigma,k} + \alpha)) \\ & - K \cos(\theta_{\sigma-1,1} - \theta_{\sigma-1,2} + \theta_{\sigma,3-k} - \theta_{\sigma,k} + \alpha) \\ & - K \cos(\theta_{\sigma-1,2} - \theta_{\sigma-1,1} + \theta_{\sigma,3-k} - \theta_{\sigma,k} + \alpha) \\ & + K \cos(\theta_{\sigma+1,1} - \theta_{\sigma+1,2} + \theta_{\sigma,3-k} - \theta_{\sigma,k} + \alpha) \\ & + K \cos(\theta_{\sigma+1,2} - \theta_{\sigma+1,1} + \theta_{\sigma,3-k} - \theta_{\sigma,k} + \alpha).\end{aligned}\tag{30}$$

Here the interactions within each population is not just given by a first harmonic as in (4) but also by a second harmonic (scaled by a parameter r); this is sometimes referred to as Hansel–Mato–Meunier coupling [147]. Moreover, the interactions between populations are not additive—as discussed in more detail below—but consist of nonlinear functions of four phase variables. It remains an open question whether such generalized interactions are necessary to generate heteroclinic dynamics between weak chimeras.

Dynamics of metastable states with localized (frequency) synchrony are of interest also in larger networks of $M > 3$ populations. Since explicit analytical results are hard to get for such networks, Shanahan [150] used numerical measures to analyze how metastable and “chimera-like” the network dynamics are. Recall that $R_\sigma(t)$ encodes the level of synchrony of population σ at time t . Let $\langle \cdot \rangle_\sigma$, Var_σ denote the mean and variance over all populations $\sigma = 1, \dots, M$ and $\langle \cdot \rangle_T$, Var_T mean and variance over the time interval $[0, T]$. Now

$$\lambda = \langle \text{Var}_T(R_\sigma(t)) \rangle_\sigma$$

gives how much synchrony of individual populations vary over time while

$$\chi = \langle \text{Var}_\sigma(R_\sigma(t)) \rangle_T$$

encodes how much synchrony varies across populations. Intuitively, large values of λ correspond to a high level of “metastability” while large values of χ indicate that the dynamics are “chimera-like”. On the one hand, these measures have subsequently been applied to more general oscillator networks [151, 152]. On the other hand, they have been applied to study the effect of changes to the network structure (for example through lesions) to the dynamics of Kuramoto–Sakaguchi oscillators (4) with additional delay on human connectome data [153].

networks of dynamical states linked by heteroclinic trajectories which allow dynamical transitions.

Networks of neuronal oscillators

Neurons can be modeled at different levels of realism and complexity [154]. However, the approach we (and many others) take is to ignore the spatial extent of individual neurons, treating each as a single point whose states are described by a small number of variables such as intracellular voltage and the concentrations of certain ions. We also ignore stochastic effects and describe the dynamics of single neurons by a small number of ordinary differential equations. The reduction of such systems to phase models in the case of weakly-coupled neurons is well-known [35] but sometimes (as below with the Theta neuron) a phase model is appropriate even without the assumption of weak coupling.

The two main types of coupling between neurons are synaptic and gap junctional. In synaptic coupling, the firing of a presynaptic neuron causes a change in the membrane conductance of the postsynaptic neuron, mediated by the release of neurotransmitters. This has the effect of causing a current to flow into the postsynaptic neuron, the current being of the form

$$I(t) = g(t)(V^{\text{rev}} - V), \quad (31)$$

where V^{rev} is the reversal potential for that synapse, V is the voltage of the postsynaptic neuron, and $g(t)$ is the time-dependent conductance. The sign of V^{rev} relative to the resting potential of the postsynaptic neuron governs whether the synapse is excitatory or inhibitory. The function $g(t)$ may be stereotypical, i.e., it may have the same functional form for each firing of the presynaptic neuron, where t is measured from the last firing, or it may have its own dynamics. One approximation in this type of modeling is to ignore the value of V in (31) and just assume that the firing of a presynaptic neuron causes a pulse of current to be injected into the postsynaptic neuron(s).

In gap junctional coupling a current flows that is proportional to voltage differences, so if neurons k and j have voltages V_k and V_j respectively and g is the (fixed) gap junction conductance, the current flowing from neuron k to neuron j is $I = (V_k - V_j)g$.

Populations of Theta neurons

In this section, we consider a population of Theta neurons (7) where the network interactions are generated by the input from all other neurons in the network. For input through synapses, for example, each neuron receives signals from the rest of the network through the input current I . Here, we will focus on the Ott–Antonsen reduction for Theta neurons (19) in the continuum limit, assuming that variations in excitability are distributed according to a Lorentzian. The key ingredient here is to write the network input in terms of the mean field variables to obtain a closed system of mean field equations; as we will see below, this is possible for a range of couplings that are relevant for neural dynamics. For now, we focus on one population and omit the population index σ .

In the following, we consider a network where each neuron emits a pulse-like signal of the form

$$P_n(\theta) = a_n(1 - \cos \theta)^n \quad (32)$$

as it fires (θ increases through π , see Figs. 6 and 2). The parameter $n \in \mathbb{N}$ determines the sharpness of a pulse and $a_n = 2^n(n!)^2/(2n)!$ is the normalization constant such that $\int_0^{2\pi} P_n(\theta) d\theta = 2\pi$; cf. Fig. 6. The average output of all neurons in the network, each one contributing identically, is

$$P^{(n)} = \frac{1}{N} \sum_{j=1}^N P_n(\theta_j). \quad (33)$$

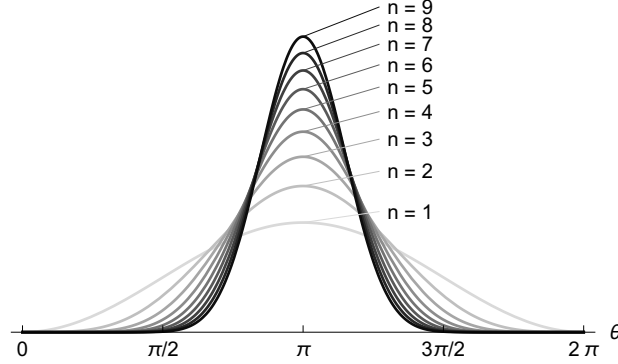


Fig 6. The function $P_n(\theta)$ is a pulse centered at $\theta = \pi$; here P_n is plotted for $n = 1, \dots, 9$. As n increases, the pulse becomes narrower.

Now $P^{(n)}$ can be expressed as a function of the order parameter Z : As shown in [76, 155, 156] we have for the continuum limit of infinitely many neurons, $N \rightarrow \infty$,

$$P^{(n)} = a_n \left(C_0 + \sum_{q=1}^n C_q (Z^q + \bar{Z}^q) \right) \quad (34)$$

with coefficients

$$C_q = \sum_{k=0}^n \sum_{m=0}^k \frac{n!(-1)^k \delta_{k-2m,q}}{2^k (n-k)! m! (k-m)!}. \quad (35)$$

Here $\delta_{p,q} = 1$ if $p = q$ and $\delta_{p,q} = 0$ otherwise. In the limit of infinitely narrow pulses, $n \rightarrow \infty$, we find

$$P^\infty = \frac{1 - |Z|^2}{1 + Z + \bar{Z} + |Z|^2}. \quad (36)$$

Synaptic coupling. If each Theta neuron (7) receives instantaneous synaptic input in the form of current pulses as in [76, 77, 155], the input current to each neuron is the network output,

$$I(t) = P^{(n)}(t). \quad (37)$$

A positive coupling strength $\kappa > 0$ for the Theta neuron (7) corresponds to excitatory coupling and $\kappa < 0$ to inhibitory coupling. Note that since I now is a function of the Kuramoto order parameter by (34), we have closed the Ott–Antonsen equation for the Theta neuron (19) to obtain a system describing the dynamics for infinitely many oscillators.

A simple modification of (7) is to add synaptic dynamics by letting the input current I satisfy the equation

$$\tau_{\text{syn}} \dot{I} = P^{(n)} - I \quad (38)$$

where τ_{syn} is the time-constant governing the synaptic dynamics. In the limit $\tau_{\text{syn}} \rightarrow 0$ the synaptic dynamics are instantaneous and we recover the previous model. Again, with (34) the Ott–Antonsen equations (19) and (38) form a closed system of equations that describe the dynamics in the continuum limit.

A single population of Theta neurons can give rise to a variety of dynamics that can be understood using the Ott–Antonsen equations: For instantaneous synaptic input, Luke *et al.* [76] found three distinct stable dynamical regimes, partially synchronous rest, partially synchronous spiking, and collective periodic wave dynamics. In partially synchronous rest most neurons remain at rest (a stable node in the two-dimensional Ott–Antonsen equations (19) for Z), in the partially synchronous spiking regime most neurons spike continuously (a stable focus for Z), and in the collective periodic wave neurons fire periodically (a stable periodic orbit of the order parameter Z). If in addition the excitability of neurons varies periodically, more complicated dynamics and macroscopic chaos appear [155].

Gap junctions. Along with synaptic coupling, the other major form of coupling between neurons is via gap junctions [157], in which a current flows between connected neurons proportional to the difference in their voltages. Using the equivalence of the Theta and QIF neuron, it was shown in [158] that adding all-to-all gap junction coupling to (7) results in the equations

$$\dot{\theta}_k = 1 - \cos \theta_k - \kappa^{\text{GJ}} \sin \theta_k + (1 + \cos \theta_k) \left(\eta_k + \kappa I + \frac{\kappa^{\text{GJ}}}{N} \sum_{j=1}^N \text{tn}(\theta_j) \right) \quad (39)$$

where κ^{GJ} is the strength of gap junction coupling and the function $\text{tn}(\theta) := \sin \theta / (1 + \cos \theta + \epsilon)$ with $0 < \epsilon \ll 1$ stems from the coordinate transformation between Theta and QIF neurons. Note that (39) is still a sinusoidally coupled system. Assuming a Lorentzian distribution of excitability η_k centered at $\hat{\eta}$ with width Δ , the dynamics in the limit of infinitely many oscillators are given by the Ott–Antonsen equation

$$\dot{Z} = \frac{1}{2} ((i\hat{\eta} - \Delta)(1 + Z)^2 - i(1 - Z)^2) + \frac{1}{2} (i(1 + Z)^2(\kappa I + \kappa^{\text{GJ}}Q) + \kappa^{\text{GJ}}(1 - Z^2)) \quad (40)$$

where

$$Q = \sum_{m=1}^{\infty} (b_m Z^m + \bar{b}_m \bar{Z}^m), \quad b_m = \frac{i(\rho^{m+1} - \rho^{m-1})}{2\sqrt{2\epsilon + \epsilon^2}}, \quad (41)$$

and $\rho \equiv \sqrt{2\epsilon + \epsilon^2} - 1 - \epsilon$. Note that the input current is still to be defined: There could be gap junction only coupling, $I = 0$, instantaneous synaptic input (37) or synaptic dynamics (38) as defined above.

The reduced equations allow, for example, to study what effect the strength of the gap junction coupling has on the dynamics. Laing [158] found that for excitatory synaptic coupling (i.e., $\kappa > 0$) increasing the strength of gap junction coupling could induce oscillations in the mean field via a Hopf bifurcation, and destroy previously existing bistability between steady states with high and low mean firing rates. For inhibitory synaptic coupling (i.e., $\kappa < 0$) increasing the strength of gap junction coupling stabilized a steady state with high mean firing rate, inducing bistability in the network. In spatially extended systems, it was found that gap junction coupling could destabilize “bump” states via a Hopf bifurcation, and create traveling waves of activity.

Conductance dynamics. The above models for Theta neurons have all assumed that synaptic coupling is via the injection of current pulses. However, Ref. [48] considers a model in which synaptic input was in the form of a current, equal to the product of a conductance and the difference between the voltage of a QIF neuron and a reversal potential V^{rev} . Converting to Theta

neuron variables, a particular case of their model can be written as

$$\dot{\theta}_k = 1 - \cos \theta_k + (1 + \cos \theta_k) (\eta_k + g(t)V^{\text{rev}}) - g(t) \sin \theta_k \quad (42)$$

with a time-dependent gating function

$$g(t) = \kappa^g P^\infty(t) \quad (43)$$

that depends on the network output modulated by the coupling strength $\kappa^g > 0$. (Note that quantities like g and V^{rev} have been non-dimensionalised by scaling relative to dimensional quantities.) The corresponding Ott–Antonsen equations read

$$\dot{Z} = \frac{1}{2} ((i\hat{\eta} - \Delta)(1 + Z)^2 - i(1 - Z)^2) + \frac{1}{2} (i(1 + Z)^2 g V^{\text{rev}} + (1 - Z^2)g) \quad (44)$$

which is closed since $g(t)$ is a function of Z by (36).

The dynamics of this network are straightforward and as expected. For inhibitory coupling ($V^{\text{rev}} < 0$) there is one stable fixed point for all $\hat{\eta}$ while for excitatory coupling ($V^{\text{rev}} > 0$) there can be a range of negative $\hat{\eta}$ values for which the network is bistable between steady states with high and low average firing rates. This bistability in an excitatorially self-coupled network is of interest as such a network can be thought of as a one-bit “memory”, stably storing one of two states.

Populations of Winfree oscillators

Although not as popular as the Kuramoto phase oscillator, the Winfree oscillator is also described by a single angular variable, and the model has a longer history [159]. Under suitable assumptions, a network of Winfree oscillators [160, 161] is amenable to simplification through the Ott–Antonsen reduction. Consider a network of N phase oscillators which evolve according to

$$\dot{\theta}_k = \omega_k + \frac{\epsilon}{N} \sum_{j=1}^N \hat{P}(\theta_j) Q(\theta_k). \quad (45)$$

for $k = 1, \dots, N$. The function Q is the phase response curve of an oscillator, which can be measured experimentally or determined from a model neuron [162]. If we set $Q(\theta) = \sin \beta - \sin(\theta + \beta)$ with parameter β then we have a sinusoidally coupled phase oscillator network. Moreover, suppose that network interaction is given by a pulsatile function $\hat{P}(\theta) = P_n(\theta - \pi)$. While \hat{P} has its maximum at $\theta = 0$ (unlike the interactions for the Theta neuron), it can be expanded in a similar way as (34) into powers of the Kuramoto order parameter. Assuming that the intrinsic frequencies are distributed as a Lorentzian, we obtain an Ott–Antonsen equation that describes the dynamics in the limit of infinitely large networks; see [161] for details.

Several groups have used this description to study the dynamics of infinite networks of Winfree oscillators. Pazó and Montbrió [161] found that such a network typically has either an asynchronous state (constant mean field) or a synchronous state (periodic oscillations in the mean field, indicating partial synchrony within the network) as attractors. They also found that varying n (the sharpness of P_n) had a significant effect on the synchronizability of the network. Laing [156] studied a spatially-extended network of Winfree oscillators and found a variety of stationary, traveling, and chaotic spatiotemporal patterns. Finally, Gallego *et al.* [163] extended the work in [161], considering a variety of types of pulsatile functions and phase response curves.

Coupled populations of neurons

While the previous sections discussed a network consisting of a single population of all-to-all coupled model neurons, an obvious generalization is to consider networks of two or more populations. Consider M populations of Theta neurons and let $P_\tau^{(n)}$ denote the output of population τ . For example for synaptic interaction amongst populations, (37) generalizes to

$$I_\sigma(t) = \sum_{\tau=1}^M \kappa_{\tau\sigma} P_\tau^{(n)}(t), \quad (46)$$

where $\kappa_{\tau\sigma}$ is the input strength from population τ to population σ . Writing each P_τ in terms of the order parameter Z_τ of population τ , we obtain a closed set of M Ott–Antonsen equations (19) that describe the dynamics for infinitely large populations.

Interacting populations of neural oscillators give rise to neural rhythms. Laing [156] considered a network of two coupled populations of Theta neurons, one inhibitory and one excitatory. Such networks support a periodic PING rhythm [164] in which the activity of both populations is periodic, with the peak activity of the excitatory population activity preceding that of the inhibitory one. Analyses of similar types of networks were performed in [43, 48, 78]. Periodic behavior of the mean-field equations of coupled populations of Theta neurons (or equivalently QIF neurons) allows one to extract macroscopic phase response curves [165] which allows treating such ensembles as single oscillatory units in weakly coupled networks.

Coupled populations of Winfree oscillators support a range of dynamics. In Ref. [161] the authors considered a symmetric pair of networks of Winfree oscillators. They observed a variety of dynamics such a quasiperiodic chimera state in which one population is perfectly synchronous while the order parameter of the other undergoes quasiperiodic oscillations. They also found a chaotic chimera state where one population is phase synchronized while the order parameter of the other one fluctuates chaotically.

Generalizations

The oscillator populations considered above do not have any sense of space themselves, apart from possibly two networks being at different points in space. The brain is three-dimensional, although the presence of layered structures could lend itself to a description in terms of a series of coupled two-dimensional domains. Regardless, the spatial aspects of neural dynamics should not be ignored. Several authors have generalized the techniques discussed above to spatial domains, deriving *neural field* models: spatiotemporal evolution equations for macroscopic quantities [77, 156, 158, 166, 167]. The main advantage of using this new generation of neural field models is that unlike classical models [168, 169], the derivations from networks of Theta neurons are exact rather than heuristic. Rather than considering neural field models on continuous spatial domains, one could consider them on a discretized network where each node is a brain region and coupling strength are given, for example, by connectome data.

All of the networks above have been all-to-all coupled which is rarely the case in real-world systems. The in-degree of a neuron is the number of neurons connecting to it, whereas the out-degree is the number of neurons to which it connects. For all-to-all coupled networks all neurons have the same in- and out-degree ($N - 1$ for a network of N neurons with no self-coupling). Several groups have considered networks in which the degrees are distributed, having a power law distribution, for example [131, 170]. The mean-field reduction techniques discussed above can be used to accurately and efficiently investigate the influence of this aspect of network structure on dynamics, and this is of great interest.

Networks of identical oscillators are described by the Watanabe–Strogatz equations. While the application to Kuramoto-type oscillator networks is fairly standard, the corresponding mean-field equations for Theta neurons (27) have only recently been studied.

Other oscillator networks

Kuramoto-type interactions

Above, we considered Kuramoto phase oscillator networks of identical populations (4) with symmetric coupling. In the following, we discuss generalizations of such networks: For example, oscillator populations which are nonidentical with intrinsic frequency distributions whose mean frequencies are distinct, $\omega_\sigma \neq \omega_{\sigma'}$ for $\sigma \neq \sigma'$. Many of the results summarized in this section are obtained using the Ott–Antonsen approach for infinitely large networks. We assume that interactions are of Kuramoto type (depending on the phase difference of pairs of oscillators); bifurcations may happen as one introduces an explicit phase dependency to the coupling [122].

Multimodal distributions of intrinsic frequencies. While Kuramoto’s original model considered a single oscillator population with unimodally distributed frequencies—such as the Lorentzian distribution—Kuramoto also speculated on what dynamic behaviors an $M = 1$ population network would exhibit if the distribution of natural frequencies was instead bimodal [64]: depending on the coupling strength, the width and spacing of the peaks of the frequency distribution, oscillators may either aggregate and form a single crowd of oscillators, thus forming one “giant oscillator,” or disintegrate into two mutually unlocked crowds, corresponding to two giant oscillators.

Crawford analyzed this case rigorously for the weakly nonlinear behavior near the incoherent state using center manifold theory [86] and thus explained local bifurcations in the neighborhood of the incoherent state. Using the Ott–Antonsen reduction, Martens *et al.* [100] obtained exact results on all possible bifurcations and the bistability between incoherent, partially synchronized, and traveling wave solutions. Similarly, rather than superimposing two unimodal frequency distributions, Pazó and Montbrió [101] considered a modified the model where the distribution of intrinsic frequencies is the difference of two Lorentzians; this allows for the central dip to become zero¹².

Interestingly, to describe a single population with an m -modal frequency distribution using the Ott–Antonsen reduction, one obtains set of m coupled ordinary differential equations. This represents the oscillator dynamics associated with each peak of the m -modes, resulting in collective behavior where oscillators either aggregate to a single or potentially up to m groups of oscillators. In the context of this review, the question arises as to whether the resulting set of equations can be related to M -population models as described by (4). This question was picked up by Pietras and Daffertshofer [172] who showed that the dynamical equations describing $M = 1$ population with a bimodal distribution can be mapped $M = 2$ populations (4) with nonidentical coupling strengths $K_{\sigma\tau}$ with equivalent bifurcations. This equivalence breaks down for $M = 3$ populations and trimodal distributions.

Chimeras for nonidentical populations. As mentioned above, chimera states appear for $M > 1$ identical populations of phase oscillators. Using the Ott–Antonsen equations, Laing showed that these dynamics persist for (4) with $M = 2$ if $\Delta_\sigma > 0$ and $\omega_\sigma \neq \omega_{\sigma'}$ in the large N

¹²The resulting frequency distribution is curiously similar to Norbert Wiener’s notion of the frequency distribution of brain waves around the alpha wave band, see, e.g., [171]

limit [129]. As heterogeneity is increased, stationary chimera states can become oscillatory through Hopf bifurcations and may eventually be entirely destroyed.

Montbrió *et al.* [173] studied two populations where not only frequencies were nonidentical ($\Delta_\sigma > 0$, $\Omega_\sigma \neq \Omega_{\sigma'}$), but also the coupling was asymmetric between the two populations. In another study, Laing *et al.* considered noncomplete networks to study the sensitivity of chimera states against gradual removal of random links starting from a complete network [131], and found that oscillations of chimera states can be either created or suppressed depending on the type of link removal.

Asymmetric input or output. Another way to break symmetry among oscillators within (or outside) a population is to lend each oscillator the intrinsic property by replacing K with a random coefficient K_j *inside* the sum in (3); oscillators with $K_j > 0$ and $K_j < 0$ thus mimic the behavior of excitatory and inhibitory neurons, respectively, and the interactions between j and j' are not necessarily symmetric, unless $K_j = K_{j'}$. The study by Hong and Strogatz [174] reveals that somewhat surprisingly, extending the Kuramoto model in this fashion yields dynamics that resembles that of the original model (3) frequencies are nonidentical frequencies, yet in the case of identical dynamics the model exhibits more complicated dynamics.

Another possibility to include coupling heterogeneity considered by the same authors is to introduce K_k *outside* of the sum in Eq. (3), thus leading to conformist/excitatory ($K_k > 0$) and contrarian/inhibitory behavior ($K_k < 0$) [175]. This setup may give rise to complex states where oscillators bunch up in groups with a phase difference of π or move like a traveling wave. A later study found that the system with identical oscillators harbors even more complex dynamics [176]. Similar coupling schemes accommodating for excitatory and inhibitory coupling have been devised for multi-population models (5), to study how solitary states emerge within a synchronized population, thus leading to the formation of clusters [177].

Generically interacting oscillators

Note that networks of Kuramoto–Sakaguchi oscillators (4) make two important assumption on the network interactions. First, the interactions are sinusoidal, as discussed above, since the coupling function has a single harmonic. Second, the network interactions are *additive* [58, 178], that is, the interaction of two distinct oscillators on a third is given by the sum of the individual interactions. By contrast, coupling between oscillatory units generically contains nonlinear (non-additive) interactions; concrete examples include interactions in ecological networks [179] and nonlinear dendritic interactions between neurons [180]. For weakly coupled oscillator networks, generic coupling results in *higher-order* interaction terms which include higher harmonics in the coupling function as well as coupling terms which depend nonlinearly on three or more oscillator phases [181]. Ashwin and Rodrigues [182] calculated these interaction terms explicitly for a globally coupled network of symmetric oscillators close to a Hopf bifurcation. These higher-order interaction terms lead to phase oscillator networks where the mean-field reductions cease to apply [114] as noted above.

Populations with distinct intrinsic frequencies

Mean-field reductions have also been successful at describing networks of nonidentical populations with distinct mean intrinsic frequencies. Resonances between the mean intrinsic frequencies give rise to higher-order interactions. Subject to certain conditions, one can apply the Ott–Antonsen reduction for the continuum limit [183] or the Watanabe–Strogatz reduction for finite networks [184] to understand the collective dynamics. If resonances between the mean intrinsic

frequencies of the populations are absent [185], then the continuum limit equations (OA)—a system with $2M$ real dimensions—simplify even further. More specifically, assume that the intrinsic frequencies are distributed according to a Lorentzian distribution with width Δ_σ and write $Z_\sigma = R_\sigma e^{i\phi_\sigma}$ for the Kuramoto order parameter as above. As outlined in [185], nonresonant interactions imply that—as in (28)—the equations for R_σ in (OA) decouple from the dynamics of the mean phases ϕ_σ . That is, the macroscopic dynamics are described by the M -dimensional system of equations

$$\dot{R}_\sigma = \left(-\Delta_\sigma - \sum_{\tau=1}^M b_{\sigma\tau} R_\tau + (1 - R_\sigma^2) \left(a_\sigma + \sum_{\tau=1}^M c_{\sigma\tau} R_\tau \right) \right) R_\sigma \quad (47)$$

where $a_\sigma, b_{\sigma\tau}, c_{\sigma\tau} \in \mathbb{R}$ are parameters which depend on the underlying nonlinear oscillator system. Note that these equations of motion are similar to Lotka–Volterra type dynamical systems which have been used to model sequential dynamics in neuroscience [145, 146]. Indeed, (47) give rise to a range of dynamical behavior including sequential localized synchronization and desynchronization through cycles of heteroclinic trajectories and chaotic dynamics [185].

Applications to large-scale neural dynamics

The theory above is particularly pertinent for the study of mesoscopic or macroscopic brain dynamics, i.e., dynamics arising from tissue that contains large populations of neurons. Such dynamics are recorded using a variety of different modalities in animal or human studies, including local field potentials (LFP) and magneto- or electroencephalographic (EEG) recordings [17]. These recording modalities sense changes in dynamics that arise in conjunction with fluctuations in populations of neurons. Thus, when recordings are taken from multiple sensors in different positions simultaneously, one can map the spatiotemporal dynamics of large regions of the brain. The inclusion of multiple sensors yields a natural way to construct a large-scale network representation of the dynamics of the brain, in which sensors are nodes of the network. Alternatively, dynamics can be attributed to distributed regions of interest within the brain, for example using approaches to solve the inverse problem and thereby reconstruct a source space network [186, 187].

Having defined nodes, to determine interactions [188] there are several ways to define the edges of large-scale brain networks; in a general context this inverse problem is known as network reconstruction [189]. Broadly speaking, edges of brain networks can be characterized as either functional, structural, or effective connections [17, 190]. In the former, a measure of statistical interrelation is used to quantify the extent that the dynamics of nodes co-evolve (see e.g. [191]), with edges linking pairs of nodes that are highly correlated being assigned large weights. Structural connectivity, on the other hand, describes a means to define edges on anatomical grounds, for example via tracing of axonal tracts [192]. Finally, edges in effective connectivity networks are defined as connection strengths in explicit dynamic models that are tuned such that dynamic recordings are well explained by the model [193].

These different ways of representing the brain in terms of networks yield several avenues for investigation that are relevant to the discussion above. Specifically, network analyses have provided insight into the mechanisms of both function and dysfunction [16, 28, 194, 195], and modeling frameworks such as those described above are required in order to explain findings and develop testable predictions [196]. A particularly pertinent question is to understand to what extent structural connectivity—the structural property of the network—shapes emergent functional connectivity—properties of the dynamics—in both healthy and disease conditions [14, 15, 17, 197–200].

Functional connectivity has been shown to be altered in myriad disorders of the brain, including epilepsy and Alzheimer’s disease [194,201–203] and is therefore becoming an important marker for brain disorders, as well as a potentially important means of understanding disease and designing therapy [16, 18]. However, in order to link different data modalities and to develop treatment, it is crucial to understand why specific changes in dynamics occur. The reduction methods described herein could help in this direction by bridging fundamental properties of neurons into emergent properties of neuronal networks, which can then be coupled to build an understanding of mesoscopic or whole-brain dynamics [3]. A recent example in this direction is an effort to use the reduced equations of the Kuramoto model to develop new closed-loop approaches for deep brain stimulation to treat patients with essential tremor and Parkinson’s disease [204].

Conclusions and open problems

The mean-field descriptions presented in this review are able to bridge spatial scales in coupled oscillator networks since they provide explicit descriptions of the macroscopic dynamics in terms of microscopic quantities. This provides explicit insights into how network coupling properties (for example, a neural connectome) relate to dynamical (and thus functional properties) of an oscillator network. Importantly, the equations are not just a black box, but tools from dynamical systems theory allow us to study explicitly how the dynamics change as network parameters are varied. We conclude by highlighting three sets of challenges for future research.

The first set of challenges relates to the reductions themselves and the mathematics behind them; some of them were already discussed in the section [*Limitations and challenges](#) and further along the way. Typically, phase oscillators that arise as weak coupling limit of are nonsinusoidal but their interaction contains higher harmonics and nonadditive terms; these may arise for example through either strongly nonlinear oscillations or nonlinear interactions between oscillators; see [181, 182] and other references above. Hence, the influence of such interactions on the mean field reductions is still to be clarified: while they could fail in certain instances [88] first results indicate that they may still provide useful information over some timescales [116]—further work in this direction is desirable. Real-world networks are often modeled as systems subject to noise. Here we point again to very recent results that extend the mean-field reductions presented here in these directions [59].

The second set of challenges concerns the relationship between the mean-field reductions, the underpinning microscopic models, and real-world data in the context of neuroscience. How do local field potentials or EEG measurements relate to the mean-field variables that constitute the reduced system equations? Connectivity can be estimated via neural imaging techniques, but how does this data relate to the coupling strength and phase-lag parameters that appear in the Ott–Antonsen equations of coupled Kuramoto–Sakaguchi populations? Or the coupling parameters of the microscopic models that are compatible with the reduction? The question becomes even more intricate for coupled populations of Theta neurons.

The last set of challenges goes well beyond the mean-field reductions presented here. Mathematical tools are helpful to describe the dynamics, but how do the dynamics map to function? How do we identify dynamics that are pathological, and use validate models of these dynamics to predict treatment responses? On the large scale, some pathologies such as epilepsy reveal salient abnormal dynamics [22], but alterations in other conditions are more subtle, and therefore model-driven analyses could be useful in the clinical context [202–204]. Insights into these fundamental questions will allow one to make the mean field reductions presented in this review even more useful to design targeted therapies for neural diseases.

Acknowledgments

We are grateful to R. Bogacz and B. Jüttner for helpful feedback on the manuscript. This article is part of the research activity of the Advanced Study Group 2017 “From Microscopic to Collective Dynamics in Neural Circuits” held at Max Planck Institute for the Physics of Complex Systems in Dresden (Germany). CB was partially funded by the People Programme (Marie Curie Actions) of the European Union’s Seventh Framework Programme (FP7/2007–2013) under REA grant agreement no. 626111. MG gratefully acknowledges the financial support of the EPSRC via grants EP/P021417/1 and EP/N014391/1. MG also acknowledges the generous support of a Wellcome Trust Institutional Strategic Support Award (<https://wellcome.ac.uk/>) via grant WT105618MA.

References

1. Winfree AT. The Geometry of Biological Time. vol. 12 of Interdisciplinary Applied Mathematics. New York, NY: Springer; 2001.
2. Strogatz SH. Exploring complex networks. *Nature*. 2001;410(6825):268–76. doi:10.1038/35065725.
3. Breakspear M. Dynamic models of large-scale brain activity. *Nature Neuroscience*. 2017;20(3). doi:10.1038/nn.4497.
4. Liu C, Weaver DR, Strogatz SH, Reppert SM. Cellular Construction of a Circadian Clock: Period Determination in the Suprachiasmatic Nuclei. *Cell*. 1997;91(6):855–860. doi:10.1016/S0092-8674(00)80473-0.
5. Buck J, Buck E. Mechanism of Rhythmic Synchronous Flashing of Fireflies: Fireflies of Southeast Asia may use anticipatory time-measuring in synchronizing their flashing. *Science*. 1968;159(3821):1319–1327. doi:10.1126/science.159.3821.1319.
6. Collins JJ, Stewart I. Coupled nonlinear oscillators and the symmetries of animal gaits. *Journal of Nonlinear Science*. 1993;3(1):349–392. doi:10.1007/BF02429870.
7. Strogatz SH, Abrams DM, McRobie A, Eckhardt B, Ott E. Theoretical mechanics: crowd synchrony on the Millennium Bridge. *Nature*. 2005;438(7064):43–4. doi:10.1038/43843a.
8. Strogatz SH, Kronauer RE, Czeisler Ca. Circadian pacemaker interferes with sleep onset at specific times each day: role in insomnia. *The American Journal of Physiology*. 1987;253(1 Pt 2):R172–8.
9. Leloup JC, Goldbeter A. Modeling the circadian clock: from molecular mechanism to physiological disorders. *BioEssays : news and reviews in molecular, cellular and developmental biology*. 2008;30(6):590–600. doi:10.1002/bies.20762.
10. Smolen P, Byrne J. Circadian Rhythm Models. *Encyclopedia of Neuroscience*. 2009;.
11. Ghosh AK, Chance B, Pye EK. Metabolic coupling and synchronization of NADH oscillations in yeast cell populations. *Arch Biochem and Biophys*. 1971;145(1). doi:10.1016/0003-9861(71)90042-7.
12. Danø S, Sørensen PG, Hynne F. Sustained oscillations in living cells. *Nature*. 1999;402(6759). doi:10.1038/46329.

13. Massie TM, Blasius B, Weithoff G, et al. Cycles, phase synchronization, and entrainment in single-species phytoplankton populations. *Proc Nat Acad Sci.* 2010;107(9). doi:10.1073/pnas.0908725107.
14. Honey CJ, Kotter R, Breakspear M, Sporns O. Network structure of cerebral cortex shapes functional connectivity on multiple time scales. *Proceedings of the National Academy of Sciences USA.* 2007;doi:10.1073/pnas.0701519104.
15. Honey CJ, Thivierge JP, Sporns O. Can structure predict function in the human brain? *NeuroImage.* 2010;52(3):766–76. doi:10.1016/j.neuroimage.2010.01.071.
16. Fornito A, Zalesky A, Breakspear M. The connectomics of brain disorders. *Nature Reviews Neuroscience.* 2015;16(3):159–172. doi:10.1038/nrn3901.
17. Bassett DS, Sporns O. Network neuroscience. *Nature Neuroscience.* 2017;20(3):353–364. doi:10.1038/nrn.4502.
18. Goodfellow M, Rummel C, Abela E, Richardson MP, Schindler K, Terry JR. Estimation of brain network ictogenicity predicts outcome from epilepsy surgery. *Scientific Reports.* 2016;6. doi:10.1038/srep29215.
19. Strogatz SH. *Sync: The emerging science of spontaneous order.* Penguin UK; 2004.
20. Glass L. Synchronization and rhythmic processes in physiology. *Nature.* 2001;410(March):277–284.
21. Dörfler F, Bullo F. Synchronization in complex networks of phase oscillators: A survey. *Automatica.* 2014;50(6):1539–1564. doi:10.1016/j.automatica.2014.04.012.
22. Kahana MJ. The Cognitive Correlates of Human Brain Oscillations. *The Journal of Neuroscience.* 2006;26(6):1669–1672. doi:10.1523/JNEUROSCI.3737-05c.2006.
23. Lehnertz K, Geier C, Rings T, Stahn K. Capturing time-varying brain dynamics. *EPJ Nonlinear Biomedical Physics.* 2017;5:2. doi:10.1051/epjnbp/2017001.
24. Fell J, Axmacher N. The role of phase synchronization in memory processes. *Nature Reviews Neuroscience.* 2011;12(2):105–118. doi:10.1038/nrn2979.
25. Fries P. Neuronal gamma-band synchronization as a fundamental process in cortical computation. *Annual Review of Neuroscience.* 2009;32:209–24. doi:10.1146/annurev.neuro.051508.135603.
26. Wang XJ. Neurophysiological and Computational Principles of Cortical Rhythms in Cognition. *Physiological Reviews.* 2010;90(3):1195–1268. doi:10.1152/physrev.00035.2008.
27. Singer W, Gray CM, Gray WS, Charles. Visual feature integration and the temporal correlation hypothesis. *Ann Rev Neurosci.* 1995;18:555–586. doi:10.1146/annurev.ne.18.030195.003011.
28. Fries P. A mechanism for cognitive dynamics: neuronal communication through neuronal coherence. *Trends in Cognitive Sciences.* 2005;9(10):474–80. doi:10.1016/j.tics.2005.08.011.
29. Marder E, Bucher D. Central pattern generators and the control of rhythmic movements. *Current Biology.* 2001;11:R986–R996. doi:10.1016/S0960-9822(01)00581-4.
30. Smith JC, Ellenberger HH, Ballanyi K, Richter DW, Feldman JL. Pre-Bötzinger Complex: A Brainstem Region That May Generate Respiratory Rhythm in Mammals. *Science.* 1991;254(5032):726–729.
31. Butera RJ, Rinzel J, Smith JC. Models of respiratory rhythm generation in the pre-Bötzinger complex. I. Bursting pacemaker neurons. *Journal Of Neurophysiology.* 1999;82(1):382–397. doi:10.1007/bf00200329.

32. Uhlhaas PJ, Singer W. Neural synchrony in brain disorders: relevance for cognitive dysfunctions and pathophysiology. *Neuron*. 2006;52(1):155–68. doi:10.1016/j.neuron.2006.09.020.
33. Hammond C, Bergman H, Brown P. Pathological synchronization in Parkinson's disease: networks, models and treatments. *Trends in Neurosciences*. 2007;30(7):357–364. doi:10.1016/j.tins.2007.05.004.
34. Rummel C, Goodfellow M, Gast H, Hauf M, Amor F, Stibal A, et al. A Systems-Level Approach to Human Epileptic Seizures. *Neuroinformatics*. 2012;doi:10.1007/s12021-012-9161-2.
35. Ashwin P, Coombes S, Nicks R. Mathematical frameworks for oscillatory network dynamics in neuroscience. *J Math Neurosc*. 2016;doi:10.1186/s13408-015-0033-6.
36. Ashwin P, Swift JW. The dynamics of n weakly coupled identical oscillators. *Journal of Nonlinear Science*. 1992;2(1):69–108. doi:10.1007/BF02429852.
37. Hansel D, Mato G, Meunier C. Phase Dynamics for Weakly Coupled Hodgkin-Huxley Neurons. *Europhysics Letters (EPL)*. 1993;23(5):367–372. doi:10.1209/0295-5075/23/5/011.
38. Hoppensteadt FC, Izhikevich EM. Weakly Connected Neural Networks. vol. 126 of *Applied Mathematical Sciences*. New York, NY: Springer; 1997.
39. Brown E, Moehlis J, Holmes P. On the Phase Reduction and Response Dynamics of Neural Oscillator Populations. *Neural Computation*. 2004;16(4):673–715. doi:10.1162/089976604322860668.
40. Nakao H. Phase reduction approach to synchronisation of nonlinear oscillators. *Contemporary Physics*. 2016;57(2):188–214. doi:10.1080/00107514.2015.1094987.
41. Monga B, Wilson D, Matchen T, Moehlis J. Phase reduction and phase-based optimal control for biological systems: a tutorial. *Biological Cybernetics*. 2018;doi:10.1007/s00422-018-0780-z.
42. Cabral J, Hugues E, Sporns O, Deco G. Role of local network oscillations in resting-state functional connectivity. *NeuroImage*. 2011;57(1):130–139. doi:10.1016/j.neuroimage.2011.04.010.
43. Luke TB, Barreto E, So P. Macroscopic complexity from an autonomous network of networks of theta neurons. *Frontiers in Computational Neuroscience*. 2014;8:145.
44. Barreto E, Hunt B, Ott E, So P. Synchronization in networks of networks: The onset of coherent collective behavior in systems of interacting populations of heterogeneous oscillators. *Physical Review E*. 2008;77(3):036107. doi:10.1103/PhysRevE.77.036107.
45. Kivelä M, Arenas A, Barthélemy M, Gleeson JP, Moreno Y, Porter MA. Multilayer networks. *Journal of Complex Networks*. 2014;2(3):203–271. doi:10.1093/comnet/cnu016.
46. Britz J, Van De Ville D, Michel CM. BOLD correlates of EEG topography reveal rapid resting-state network dynamics. *NeuroImage*. 2010;52(4):1162–1170. doi:10.1016/j.neuroimage.2010.02.052.
47. Izhikevich EM. *Dynamical systems in neuroscience: The geometry of excitability and bursting*. The MIT press; 2007.
48. Coombes S, Byrne Á. Next Generation Neural Mass Models. In: Corinto F, Torcini A, editors. *Nonlinear Dynamics in Computational Neuroscience*. Springer, Cham; 2019. p. 1–16.
49. Panaggio MJ, Abrams DM. Chimera states: coexistence of coherence and incoherence in networks of coupled oscillators. *Nonlinearity*. 2015;28(3):R67. doi:10.1088/0951-7715/28/3/R67.
50. Schöll E. Synchronization patterns and chimera states in complex networks: Interplay of topology and dynamics. *The European Physical Journal Special Topics*. 2016;225(6-7):891–919. doi:10.1140/epjst/e2016-02646-3.

51. Omel'chenko OE. The mathematics behind chimera states. *Nonlinearity*. 2018;31(5):R121–R164. doi:10.1088/1361-6544/aaaa07.
52. Porter M, Gleeson J. *Dynamical Systems on Networks*. vol. 4 of *Frontiers in Applied Dynamical Systems: Reviews and Tutorials*. Cham: Springer International Publishing; 2016.
53. Rodrigues FA, Peron TKD, Ji P, Kurths J. The Kuramoto model in complex networks. *Physics Reports*. 2016;610:1–98. doi:10.1016/j.physrep.2015.10.008.
54. Pecora LM, Carroll TL. Master Stability Functions for Synchronized Coupled Systems. *Physical Review Letters*. 1998;80(10):2109–2112. doi:10.1103/PhysRevLett.80.2109.
55. Barahona M, Pecora LM. Synchronization in Small-World Systems. *Physical Review Letters*. 2002;89(5):054101. doi:10.1103/PhysRevLett.89.054101.
56. Pereira T, Eldering J, Rasmussen M, Veneziani A. Towards a theory for diffusive coupling functions allowing persistent synchronization. *Nonlinearity*. 2014;27(3):501–525. doi:10.1088/0951-7715/27/3/501.
57. Holme P, Saramäki J. Temporal networks. *Physics Reports*. 2012;519:97–125. doi:10.1016/j.physrep.2012.03.001.
58. Bick C, Field MJ. Asynchronous networks and event driven dynamics. *Nonlinearity*. 2017;30(2):558–594. doi:10.1088/1361-6544/aa4f62.
59. Tyulkina IV, Goldobin DS, Klimenko LS, Pikovsky A. Dynamics of Noisy Oscillator Populations beyond the Ott-Antonsen Ansatz. *Phys Rev Lett*. 2018;120:264101. doi:10.1103/PhysRevLett.120.264101.
60. Gottwald GA. Model reduction for networks of coupled oscillators. *Chaos*. 2015;25(5):053111. doi:10.1063/1.4921295.
61. Skardal PS, Restrepo JG, Ott E. Uncovering low dimensional macroscopic chaotic dynamics of large finite size complex systems. *Chaos*. 2017;27:083121. doi:10.1063/1.4986957.
62. Hannay KM, Forger DB, Booth V. Macroscopic models for networks of coupled biological oscillators. *Science Advances*. 2018;4(8):e1701047. doi:10.1126/sciadv.1701047.
63. Fawcett TW, Higginson AD. Heavy use of equations impedes communication among biologists. *Proceedings of the National Academy of Sciences USA*. 2012;109(29):11735–11739. doi:10.1073/pnas.1205259109.
64. Kuramoto Y. *Chemical oscillations, waves, and turbulence*. Springer-Verlag, New York; 1984.
65. Strogatz SH. From Kuramoto to Crawford: exploring the onset of synchronization in populations of coupled oscillators. *Physica D*. 2000;143:1–20. doi:10.1016/S0167-2789(00)00094-4.
66. Sakaguchi H, Kuramoto Y. A Soluble Active Rotator Model Showing Phase Transitions via Mutual Entertainment. *Progress of Theoretical Physics*. 1986;76(3):576–581. doi:10.1143/PTP.76.576.
67. Swift JW, Strogatz SH, Wiesenfeld K. Averaging of globally coupled oscillators. *Physica D*. 1992;55(3-4):239–250. doi:10.1016/0167-2789(92)90057-T.
68. Cumin D, Unsworth CP. Generalising the Kuramoto model for the study of neuronal synchronisation in the brain. *Physica D*. 2007;226(2):181–196.
69. Breakspear M, Heitmann S, Daffertshofer A. Generative models of cortical oscillations: neurobiological implications of the Kuramoto model. *Frontiers in Human Neuroscience*. 2010;4:190.

70. Schmidt H, Petkov G, Richardson MP, Terry JR. Dynamics on Networks: The Role of Local Dynamics and Global Networks on the Emergence of Hypersynchronous Neural Activity. *PLoS Computational Biology*. 2014;10(11):e1003947. doi:10.1371/journal.pcbi.1003947.
71. Ermentrout GB. Ermentrout-Kopell canonical model. *Scholarpedia*. 2008;3(3):1398. doi:10.4249/scholarpedia.1398.
72. Ermentrout GB, Kopell N. Parabolic bursting in an excitable system coupled with a slow oscillation. *SIAM Journal on Applied Mathematics*. 1986;46(2):233–253.
73. Monteforte M, Wolf F. Dynamical Entropy Production in Spiking Neuron Networks in the Balanced State. *Physical Review Letters*. 2010;105(26):268104. doi:10.1103/PhysRevLett.105.268104.
74. Osan R, Ermentrout GB. Two dimensional synaptically generated traveling waves in a theta-neuron neural network. *Neurocomputing*. 2001;38:789–795.
75. Ermentrout GB, Rubin J, Osan R. Regular traveling waves in a one-dimensional network of theta neurons. *SIAM Journal on Applied Mathematics*. 2002;62(4):1197–1221.
76. Luke TB, Barreto E, So P. Complete Classification of the Macroscopic Behavior of a Heterogeneous Network of Theta Neurons. *Neural Computation*. 2013;25(12):3207–3234. doi:10.1162/NECO_a.00525.
77. Laing CR. Derivation of a neural field model from a network of theta neurons. *Physical Review E*. 2014;90(1):010901. doi:10.1103/PhysRevE.90.010901.
78. Montbrió E, Pazó D, Roxin A. Macroscopic Description for Networks of Spiking Neurons. *Physical Review X*. 2015;5(2):021028. doi:10.1103/PhysRevX.5.021028.
79. Gutkin B. Theta Neuron Model. *Encyclopedia of Computational Neuroscience*. 2015; p. 2958–2965.
80. Kopell N, Ermentrout GB. Chemical and electrical synapses perform complementary roles in the synchronization of interneuronal networks. *Proceedings of the National Academy of Sciences USA*. 2004;101(43):15482–15487.
81. Brunel N, Latham PE. Firing rate of the noisy quadratic integrate-and-fire neuron. *Neural Computation*. 2003;15(10):2281–2306.
82. Latham PE, Richmond B, Nelson P, Nirenberg S. Intrinsic dynamics in neuronal networks. I. Theory. *Journal of Neurophysiology*. 2000;83(2):808–827.
83. Hansel D, Mato G. Existence and stability of persistent states in large neuronal networks. *Physical Review Letters*. 2001;86(18):4175.
84. Pietras B, Daffertshofer A. Ott-Antonsen attractiveness for parameter-dependent oscillatory systems. *Chaos*. 2016;26(10):103101. doi:10.1063/1.4963371.
85. Sakaguchi H. Cooperative Phenomena in Coupled Oscillator Systems under External Fields. *Progress of Theoretical Physics*. 1988;79(1):39–46. doi:10.1143/PTP.79.39.
86. Crawford JD. Amplitude expansions for instabilities in populations of globally-coupled oscillators. *Journal of Statistical Physics*. 1994;74(5):1047–1084.
87. Acebrón J, Bonilla L, Pérez Vicente C, et al. The Kuramoto model: A simple paradigm for synchronization phenomena. *Rev Mod Physics*. 2005;77(1). doi:10.1103/RevModPhys.77.137.

88. Lai YM, Porter MA. Noise-induced synchronization, desynchronization, and clustering in globally coupled nonidentical oscillators. *Physical Review E*. 2013;88(1):012905. doi:10.1103/PhysRevE.88.012905.
89. Landau L, Lifshitz E. *Course of theoretical physics*. vol. 6: Fluid mechanics. London; 1959.
90. Strogatz SH, Mirollo RE. Stability of incoherence in a population of coupled oscillators. *Journal of Statistical Physics*. 1991;63(3-4):613–635. doi:10.1007/BF01029202.
91. Lancellotti C. On the Vlasov Limit for Systems of Nonlinearly Coupled Oscillators without Noise. *Transport Theory and Statistical Physics*. 2005;34(7):523–535. doi:10.1080/00411450508951152.
92. Mirollo RE, Strogatz SH. The Spectrum of the Partially Locked State for the Kuramoto Model. *Journal of Nonlinear Science*. 2007;17(4):309–347. doi:10.1007/s00332-006-0806-x.
93. Carrillo JA, Choi YP, Ha SY, Kang MJ, Kim Y. Contractivity of Transport Distances for the Kinetic Kuramoto Equation. *Journal of Statistical Physics*. 2014;156(2):395–415. doi:10.1007/s10955-014-1005-z.
94. Dietert H. Stability and bifurcation for the Kuramoto model. *Journal de Mathématiques Pures et Appliquées*. 2016;105(4):451–489. doi:10.1016/j.matpur.2015.11.001.
95. Dietert H, Fernandez B, David GV. Landau damping to partially locked states in the Kuramoto model. arXiv:160604470. 2016; p. 1–29.
96. Chiba H, Medvedev GS. The mean field analysis for the Kuramoto model on graphs I. The mean field equation and transition point formulas. arXiv:161206493. 2016; p. 1–29.
97. Ott E, Antonsen TM. Low dimensional behavior of large systems of globally coupled oscillators. *Chaos*. 2008;18(3):037113. doi:10.1063/1.2930766.
98. Ott E, Antonsen TM. Long time evolution of phase oscillator systems. *Chaos*. 2009;19(2):023117. doi:10.1063/1.3136851.
99. Ott E, Hunt BR, Antonsen TM. Comment on “Long time evolution of phase oscillator systems” [Chaos 19, 023117 (2009)]. *Chaos*. 2011;21(2):025112. doi:10.1063/1.3574931.
100. Martens EA, Barreto E, Strogatz SH, Ott E, So P, Antonsen TM. Exact results for the Kuramoto model with a bimodal frequency distribution. *Physical Review E*. 2009;79(2):026204. doi:10.1103/PhysRevE.79.026204.
101. Pazó D, Montbrió E. Existence of hysteresis in the Kuramoto model with bimodal frequency distributions. *Physical Review E*. 2009;80(4):046215. doi:10.1103/PhysRevE.80.046215.
102. Tsang KY, Mirollo RE, Strogatz SH, Wiesenfeld K. Dynamics of a globally coupled oscillator array. *Physica D*. 1991;48(1):102–112. doi:10.1016/0167-2789(91)90054-D.
103. Wiesenfeld K, Colet P, Strogatz SH. Frequency locking in Josephson arrays: Connection with the Kuramoto model. *Physical Review E*. 1998;57(2):1563–1569. doi:10.1103/PhysRevE.57.1563.
104. Watanabe S, Strogatz SH. Integrability of a globally coupled oscillator array. *Physical Review Letters*. 1993;70(16):2391–2394. doi:10.1103/PhysRevLett.70.2391.
105. Watanabe S, Strogatz SH. Constants of motion for superconducting Josephson arrays. *Physica D*. 1994;74(3-4):197–253. doi:10.1016/0167-2789(94)90196-1.
106. Goebel CJ. Comment on Constants of motion for superconductor arrays. *Physica D*. 1995;80(1-2):18–20. doi:10.1016/0167-2789(95)90049-7.

107. Marvel SA, Mirollo RE, Strogatz SH. Identical phase oscillators with global sinusoidal coupling evolve by Möbius group action. *Chaos*. 2009;19(4):043104. doi:10.1063/1.3247089.
108. Stewart I. Phase Oscillators With Sinusoidal Coupling Interpreted in Terms of Projective Geometry. *International Journal of Bifurcation and Chaos*. 2011;21(06):1795–1804. doi:10.1142/S0218127411029446.
109. Chen B, Engelbrecht JR, Mirollo RE. Hyperbolic geometry of Kuramoto oscillator networks. *Journal of Physics A: Mathematical and Theoretical*. 2017;50(35):355101. doi:10.1088/1751-8121/aa7e39.
110. Pikovsky A, Rosenblum M. Dynamics of heterogeneous oscillator ensembles in terms of collective variables. *Physica D*. 2011;240(9-10):872–881. doi:10.1016/j.physd.2011.01.002.
111. Pikovsky A, Rosenblum M. Partially integrable dynamics of hierarchical populations of coupled oscillators. *Phys Rev Lett*. 2008;101:264103. doi:10.1103/PhysRevLett.101.264103.
112. Laing CR. The Dynamics of Networks of Identical Theta Neurons. *The Journal of Mathematical Neuroscience*. 2018;8(1):4.
113. Bick C, Timme M, Paulikat D, Rathlev D, Ashwin P. Chaos in Symmetric Phase Oscillator Networks. *Physical Review Letters*. 2011;107(24):244101. doi:10.1103/PhysRevLett.107.244101.
114. Bick C, Ashwin P, Rodrigues A. Chaos in generically coupled phase oscillator networks with nonpairwise interactions. *Chaos*. 2016;26(9):094814. doi:10.1063/1.4958928.
115. Ashwin P, Bick C, Burylko O. Identical Phase Oscillator Networks: Bifurcations, Symmetry and Reversibility for Generalized Coupling. *Frontiers in Applied Mathematics and Statistics*. 2016;2(7). doi:10.3389/fams.2016.00007.
116. Vlasov V, Rosenblum M, Pikovsky A. Dynamics of weakly inhomogeneous oscillator populations: perturbation theory on top of Watanabe-Strogatz integrability. *Journal of Physics A: Mathematical and Theoretical*. 2016;49(31):31LT02. doi:10.1088/1751-8113/49/31/31LT02.
117. Mirollo RE. The asymptotic behavior of the order parameter for the infinite-N Kuramoto model. *Chaos*. 2012;22(4):043118. doi:10.1063/1.4766596.
118. Golubitsky M, Stewart I. The Symmetry Perspective. vol. 200 of *Progress in Mathematics*. Basel: Birkhäuser Verlag; 2002.
119. Kemeth FP, Haugland SW, Schmidt L, Kevrekidis IG, Krischer K. A classification scheme for chimera states. *Chaos*. 2016;26:094815. doi:10.1063/1.4959804.
120. Kemeth FP, Haugland SW, Krischer K. Symmetries of Chimera States. *Physical Review Letters*. 2018;120(21):214101. doi:10.1103/PhysRevLett.120.214101.
121. Kuramoto Y, Battogtokh D. Coexistence of coherence and incoherence in nonlocally coupled phase oscillators. *Nonlin Phenom in Comp Sys*. 2002;4:380–385.
122. Brown E, Holmes P, Moehlis J. Globally coupled oscillator networks. In: *Perspectives and Problems in Nonlinear Science: A Celebratory Volume in Honor of Larry Sirovich*. Springer; 2003. p. 183–215.
123. Pikovsky A, Rosenblum M. Dynamics of globally coupled oscillators: Progress and perspectives. *Chaos*. 2015;25(9):097616. doi:10.1063/1.4922971.
124. Lohe MA. The WS transform for the Kuramoto model with distributed amplitudes, phase lag and time delay. *Journal of Physics A: Mathematical and Theoretical*. 2017;50(50):505101. doi:10.1088/1751-8121/aa98ef.

125. Schwartz AJ. A Generalization of a Poincaré-Bendixson Theorem to Closed Two-Dimensional Manifolds. *American Journal of Mathematics*. 1963;85(3):453. doi:10.2307/2373135.
126. Martens EA, Bick C, Panaggio MJ. Chimera states in two populations with heterogeneous phase-lag. *Chaos*. 2016;26(9):094819. doi:10.1063/1.4958930.
127. Abrams DM, Mirollo RE, Strogatz SH, Wiley DA. Solvable Model for Chimera States of Coupled Oscillators. *Physical Review Letters*. 2008;101(8):084103. doi:10.1103/PhysRevLett.101.084103.
128. Martens EA, Panaggio MJ, Abrams DM. Basins of attraction for chimera states. *New Journal of Physics*. 2016;18(2):022002. doi:10.1088/1367-2630/18/2/022002.
129. Laing CR. Chimera states in heterogeneous networks. *Chaos*. 2009;19(1):013113. doi:10.1063/1.3068353.
130. Laing CR. Disorder-induced dynamics in a pair of coupled heterogeneous phase oscillator networks. *Chaos*. 2012;22(4):043104. doi:10.1063/1.4758814.
131. Laing CR, Rajendran K, Kevrekidis IG. Chimeras in random non-complete networks of phase oscillators. *Chaos*. 2012;22(1):013132. doi:10.1063/1.3694118.
132. Choe CU, Ri JS, Kim RS. Incoherent chimera and glassy states in coupled oscillators with frustrated interactions. *Physical Review E*. 2016;94(3):032205. doi:10.1103/PhysRevE.94.032205.
133. Bick C, Panaggio MJ, Martens EA. Chaos in Kuramoto oscillator networks. *Chaos*. 2018;28(7):071102. doi:10.1063/1.5041444.
134. Panaggio MJ, Abrams DM, Ashwin P, Laing CR. Chimera states in networks of phase oscillators: The case of two small populations. *Physical Review E*. 2016;93(1):012218. doi:10.1103/PhysRevE.93.012218.
135. Ashwin P, Burylko O. Weak chimeras in minimal networks of coupled phase oscillators. *Chaos*. 2015;25:013106. doi:10.1063/1.4905197.
136. Bick C, Ashwin P. Chaotic weak chimeras and their persistence in coupled populations of phase oscillators. *Nonlinearity*. 2016;29(5):1468–1486. doi:10.1088/0951-7715/29/5/1468.
137. Bick C. Isotropy of Angular Frequencies and Weak Chimeras with Broken Symmetry. *Journal of Nonlinear Science*. 2017;27(2):605–626. doi:10.1007/s00332-016-9345-2.
138. Bick C, Sebek M, Kiss IZ. Robust Weak Chimeras in Oscillator Networks with Delayed Linear and Quadratic Interactions. *Physical Review Letters*. 2017;119(16):168301. doi:10.1103/PhysRevLett.119.168301.
139. Martens EA. Bistable chimera attractors on a triangular network of oscillator populations. *Physical Review E*. 2010;82(1):016216. doi:10.1103/PhysRevE.82.016216.
140. Martens EA. Chimeras in a network of three oscillator populations with varying network topology. *Chaos*. 2010;20(4):043122. doi:10.1063/1.3499502.
141. Abeles M, Bergman H, Gat I, Meilijson I, Seidemann E, Tishby N, et al. Cortical activity flips among quasi-stationary states. *Proceedings of the National Academy of Sciences USA*. 1995;92(19):8616–8620.
142. Tognoli E, Kelso JAS. The Metastable Brain. *Neuron*. 2014;81(1):35–48. doi:10.1016/j.neuron.2013.12.022.

143. Ashwin P, Timme M. Nonlinear dynamics: When instability makes sense. *Nature*. 2005;436(7047):36–37. doi:10.1038/436036b.
144. Weinberger O, Ashwin P. From coupled networks of systems to networks of states in phase space. *Discrete & Continuous Dynamical Systems - B*. 2018;23(5):2043–2063. doi:10.3934/dcdsb.2018193.
145. Rabinovich MI, Varona P, Selverston A, Abarbanel HDI. Dynamical principles in neuroscience. *Reviews of Modern Physics*. 2006;78(4):1213–1265. doi:10.1103/RevModPhys.78.1213.
146. Rabinovich MI, Afraimovich VS, Bick C, Varona P. Information flow dynamics in the brain. *Physics of Life Reviews*. 2012;9(1):51–73. doi:10.1016/j.plrev.2011.11.002.
147. Hansel D, Mato G, Meunier C. Clustering and slow switching in globally coupled phase oscillators. *Physical Review E*. 1993;48(5):3470–3477.
148. Ashwin P, Orosz G, Wordsworth J, Townley S. Dynamics on Networks of Cluster States for Globally Coupled Phase Oscillators. *SIAM Journal on Applied Dynamical Systems*. 2007;6(4):728. doi:10.1137/070683969.
149. Bick C. Heteroclinic switching between chimeras. *Physical Review E*. 2018;97(5):050201. doi:10.1103/PhysRevE.97.050201.
150. Shanahan M. Metastable chimera states in community-structured oscillator networks. *Chaos*. 2010;20(1):013108. doi:10.1063/1.3305451.
151. Wildie M, Shanahan M. Metastability and chimera states in modular delay and pulse-coupled oscillator networks. *Chaos*. 2012;22(4):043131. doi:10.1063/1.4766592.
152. Deco G, Cabral J, Woolrich MW, Stevner ABA, van Hartevelt TJ, Kringelbach ML. Single or multiple frequency generators in on-going brain activity: A mechanistic whole-brain model of empirical MEG data. *NeuroImage*. 2017;152(March):538–550. doi:10.1016/j.neuroimage.2017.03.023.
153. Park HJ, Friston K. Structural and functional brain networks: From connections to cognition. *Science*. 2013;342(6158). doi:10.1126/science.1238411.
154. Koch C. *Biophysics of computation: information processing in single neurons*. Oxford University Press; 2004.
155. So P, Luke TB, Barreto E. Networks of theta neurons with time-varying excitability: Macroscopic chaos, multistability, and final-state uncertainty. *Physica D*. 2014;267:16–26.
156. Laing CR. Phase oscillator network models of brain dynamics. In: Moustafa AA, editor. *Computational Models of Brain and Behavior*. Wiley-Blackwell; 2017. p. 505–518.
157. Coombes S. Neuronal networks with gap junctions: A study of piecewise linear planar neuron models. *SIAM Journal on Applied Dynamical Systems*. 2008;7(3):1101–1129.
158. Laing CR. Exact neural fields incorporating gap junctions. *SIAM Journal on Applied Dynamical Systems*. 2015;14(4):1899–1929.
159. Winfree AT. Biological rhythms and the behavior of populations of coupled oscillators. *Journal of Theoretical Biology*. 1967;16(1):15–42.
160. Ariaratnam JT, Strogatz SH. Phase diagram for the Winfree model of coupled nonlinear oscillators. *Physical Review Letters*. 2001;86(19):4278.
161. Pazó D, Montbrió E. Low-Dimensional Dynamics of Populations of Pulse-Coupled Oscillators. *Physical Review X*. 2014;4(1):011009. doi:10.1103/PhysRevX.4.011009.

162. Schultheiss NW, Prinz AA, Butera RJ. Phase response curves in neuroscience: theory, experiment, and analysis. Springer Science & Business Media; 2011.
163. Gallego R, Montbrió E, Pazó D. Synchronization scenarios in the Winfree model of coupled oscillators. *Physical Review E*. 2017;96(4):042208.
164. Börgers C, Kopell N. Synchronization in networks of excitatory and inhibitory neurons with sparse, random connectivity. *Neural Computation*. 2003;15(3):509–538.
165. Dumont G, Ermentrout GB, Gutkin B. Macroscopic phase-resetting curves for spiking neural networks. *Physical Review E*. 2017;96(4):042311. doi:10.1103/PhysRevE.96.042311.
166. Laing CR. Travelling waves in arrays of delay-coupled phase oscillators. *Chaos*. 2016;26(9):094802.
167. Esnaola-Acebes JM, Roxin A, Avitabile D, Montbrió E. Synchrony-induced modes of oscillation of a neural field model. *Physical Review E*. 2017;96(5):052407.
168. Wilson HR, Cowan JD. A mathematical theory of the functional dynamics of cortical and thalamic nervous tissue. *Biological Cybernetics*. 1973;13(2):55–80.
169. Amari Si. Dynamics of pattern formation in lateral-inhibition type neural fields. *Biological Cybernetics*. 1977;27(2):77–87.
170. Chandra S, Hathcock D, Crain K, Antonsen TM, Girvan M, Ott E. Modeling the network dynamics of pulse-coupled neurons. *Chaos*. 2017;27(3):033102.
171. Strogatz SH. Norbert Wiener's brain waves. In: *Frontiers in Mathematical Biology: Lecture Notes in Biomathematics*, Vol. 100. vol. 100. Springer; 1994. p. 122–122.
172. Pietras B, Deschle N, Daffertshofer A. Equivalence of coupled networks and networks with multimodal frequency distributions: Conditions for the bimodal and trimodal case. *Physical Review E*. 2016;94(5):052211. doi:10.1103/PhysRevE.94.052211.
173. Montbrió E, Kurths J, Blasius B. Synchronization of two interacting populations of oscillators. *Physical Review E*. 2004;70(5):56125.
174. Hong H, Strogatz SH. Mean-field behavior in coupled oscillators with attractive and repulsive interactions. *Physical Review E*. 2012;85(5):056210. doi:10.1103/PhysRevE.85.056210.
175. Hong H, Strogatz SH. Kuramoto Model of Coupled Oscillators with Positive and Negative Coupling Parameters: An Example of Conformist and Contrarian Oscillators. *Physical Review Letters*. 2011;106(5):1–4. doi:10.1103/PhysRevLett.106.054102.
176. Hong H, Strogatz SH. Conformists and contrarians in a Kuramoto model with identical natural frequencies. *Physical Review E*. 2011;84(4):1–6. doi:10.1103/PhysRevE.84.046202.
177. Maistrenko YL, Penkovsky B, Rosenblum M. Solitary state at the edge of synchrony in ensembles with attractive and repulsive interactions. *Physical Review E*. 2014;89(6):060901. doi:10.1103/PhysRevE.89.060901.
178. Aguiar MAD, Dias APS. Synchronization and equitable partitions in weighted networks. *Chaos*. 2018;28(7):073105. doi:10.1063/1.4997385.
179. Levine JM, Bascompte J, Adler PB, Allesina S. Beyond pairwise mechanisms of species coexistence in complex communities. *Nature*. 2017;546(7656):56–64. doi:10.1038/nature22898.
180. Polsky A, Mel BW, Schiller J. Computational subunits in thin dendrites of pyramidal cells. *Nature Neuroscience*. 2004;7(6):621–627. doi:10.1038/nn1253.

181. Rosenblum M, Pikovsky A. Self-Organized Quasiperiodicity in Oscillator Ensembles with Global Nonlinear Coupling. *Physical Review Letters*. 2007;98(6):064101. doi:10.1103/PhysRevLett.98.064101.
182. Ashwin P, Rodrigues A. Hopf normal form with S_N symmetry and reduction to systems of nonlinearly coupled phase oscillators. *Physica D*. 2016;325:14–24. doi:10.1016/j.physd.2016.02.009.
183. Komarov MA, Pikovsky A. Dynamics of Multifrequency Oscillator Communities. *Physical Review Letters*. 2013;110(13):134101. doi:10.1103/PhysRevLett.110.134101.
184. Lück S, Pikovsky A. Dynamics of multi-frequency oscillator ensembles with resonant coupling. *Physics Letters A*. 2011;375(28-29):2714–2719. doi:10.1016/j.physleta.2011.06.016.
185. Komarov MA, Pikovsky A. Effects of nonresonant interaction in ensembles of phase oscillators. *Physical Review E*. 2011;84(1):016210. doi:10.1103/PhysRevE.84.016210.
186. Jonmohamadi Y, Poudel G, Innes C, Jones R. Source-space ICA for EEG source separation, localization, and time-course reconstruction. *NeuroImage*. 2014;101:720–737. doi:10.1016/j.neuroimage.2014.07.052.
187. Hassan M, Dufor O, Merlet I, Berrou C, Wendling F. EEG source connectivity analysis: From dense array recordings to brain networks. *PLoS ONE*. 2014;9(8). doi:10.1371/journal.pone.0105041.
188. Stankovski T, Pereira T, McClintock PVE, Stefanovska A. Coupling functions: Universal insights into dynamical interaction mechanisms. *Reviews of Modern Physics*. 2017;89(4):045001. doi:10.1103/RevModPhys.89.045001.
189. Timme M, Casadiego J. Revealing networks from dynamics: an introduction. *Journal of Physics A: Mathematical and ...* 2014;47:1–37.
190. Friston KJ. Functional and effective connectivity: a review. *Brain Connectivity*. 2011;1(1):13–36. doi:10.1089/brain.2011.0008.
191. Wang HE, Friston KJ, Bénar CG, Woodman MM, Chauvel P, Jirsa V, et al. MULAN: Evaluation and ensemble statistical inference for functional connectivity. *NeuroImage*. 2018;166(October 2017):167–184. doi:10.1016/j.neuroimage.2017.10.036.
192. Garcés P, Pereda E, Hernández-Tamames JA, Del-Pozo F, Maestú F, Ángel Pineda-Pardo J. Multimodal description of whole brain connectivity: A comparison of resting state MEG, fMRI, and DWI. *Human Brain Mapping*. 2016;37(1):20–34. doi:10.1002/hbm.22995.
193. Valdes-Sosa PA, Roebroeck A, Daunizeau J, Friston K. Effective connectivity: Influence, causality and biophysical modeling. *NeuroImage*. 2011;58(2):339–361. doi:10.1016/j.neuroimage.2011.03.058.
194. Stam CJ. Modern network science of neurological disorders. *Nature Reviews Neuroscience*. 2014;15(10):683–695. doi:10.1038/nrn3801.
195. Bastos AM, Vezoli J, Fries P. Communication through coherence with inter-areal delays. *Current Opinion in Neurobiology*. 2015;31:173–180. doi:10.1016/j.conb.2014.11.001.
196. Bassett DS, Zurn P, Gold JI. On the nature and use of models in network neuroscience. *Nature Reviews Neuroscience*. 2018;19(9):566–578. doi:10.1038/s41583-018-0038-8.
197. Senden M, Deco G, De Reus MA, Goebel R, Van Den Heuvel MP. Rich club organization supports a diverse set of functional network configurations. *NeuroImage*. 2014;96:174–182. doi:10.1016/j.neuroimage.2014.03.066.

198. Demirtaş M, Falcon C, Tucholka A, Gispert JD, Molinuevo JL, Deco G. A whole-brain computational modeling approach to explain the alterations in resting-state functional connectivity during progression of Alzheimer's disease. *NeuroImage: Clinical*. 2017;16(August):343–354. doi:10.1016/j.nicl.2017.08.006.
199. Misić B, Betzel RF, Reus MAD, Heuvel MPVD, Berman MG, McIntosh AR, et al. Network-Level Structure-Function Relationships in Human Neocortex. *Cerebral Cortex*. 2016;26(July):3285–3296. doi:10.1093/cercor/bhw089.
200. Shen K, Hutchison RM, Bezgin G, Everling S, McIntosh AR. Network Structure Shapes Spontaneous Functional Connectivity Dynamics. *The Journal of Neuroscience*. 2015;35(14):5579–5588. doi:10.1523/JNEUROSCI.4903-14.2015.
201. Dauwels J, Vialatte F, Musha T, Cichocki A. A comparative study of synchrony measures for the early diagnosis of Alzheimer's disease based on EEG. *NeuroImage*. 2010;49(1):668–693. doi:10.1016/j.neuroimage.2009.06.056.
202. Schmidt H, Woldman W, Goodfellow M, Chowdhury FA, Koutroumanidis M, Jewell S, et al. A computational biomarker of idiopathic generalized epilepsy from resting state EEG. *Epilepsia*. 2016;57(10):e200–e204. doi:10.1111/epi.13481.
203. Tait L, Goodfellow M, et al. under review - to be updated. Submitted. 2019;.
204. Weerasinghe G, Duchet B, Cagnan H, Brown P, Bick C, Bogacz R. Predicting the effects of deep brain stimulation using a reduced coupled oscillator model. *bioRxiv*:448290. 2018;doi:10.1101/448290.